CHAPTER III

LUMINESCENCE MOLECULAR LOGIC GATES

3.1 Introduction

3.1.1 Membranes and surfactants[61-63]

Biological membranes are very important in nature as they are able to organize living matter in cells, create a fluid two-dimensional matrix and allow for the controlled transport of solutes. Many important processes which occur in biology are membrane mediated, yet surprisingly little is known about both these reactions and more importantly, the complex nanoenvironments in which these reactions occur.

Surfactant is aggregated of surfactant molecule dispersed in a liquid colloid. Normally, a surfactant in aqueous solution forms an aggregation with the hydrophilic "head" regions in contact with surrounding solvent, sequestering the hydrophobic tailregions in the surfactant centre. The typical surfactant is known as a normal phase surfactant (oil-in-water surfactant). Inverse surfactants have the headgroups at the centre with the tails extending out (water-in-oil surfactant). The shape and size of a surfactant is a function of the molecular geometry of its surfactant molecules and solution conditions such as surfactant concentration, temperature, pH, and ionic strength.

a) b)

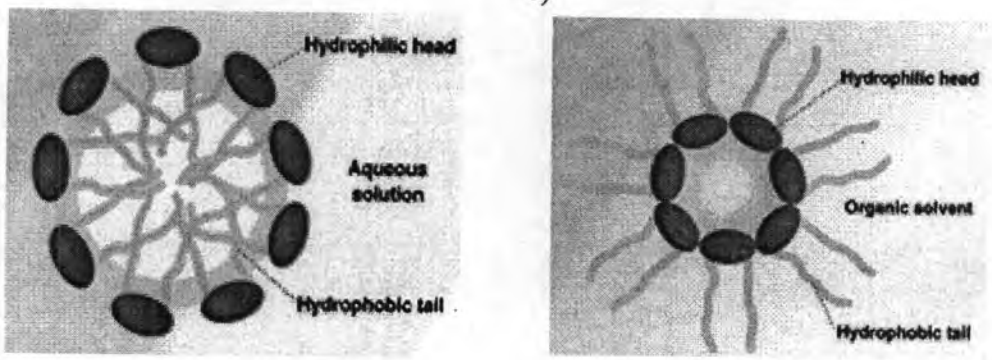

Figure 3.1 a) a surfactant formed by phospholipids in an aqueous solution.
b) an inverse surfactant formed by phospholipids in an organic solvent.

3.1.2 Self-assembling in surfactant aggregates[64]

When lipophilic ligands and fluorophore molecules dispersed in an aqueous solution containing surfactants, they move into the surfactant aggregates to generate a co-micellar assembly. The main advantages of such a system are:

1. selectivity, mainly due to the ligand choice.

2. simplicity: the sole mixing of the component in water is required to prepare the sensor.

3. the possibility to tone the detection range just by the modification of the components ratio.

4. modularity, which allows the modification or the optimization of the system by simply substituting one of the components.

3.1.3 Molecular Computational Identification (MCID)

MCID is a technique in which molecules are used as means for identifying individual cells or other small objects.[65] Using the great variety of logic types, input chemical combinations, switching and even gate arrays in addition to colours, it is possible to produce unique identifiers for members of populations of small polymer beads. It is therefore simple to understand why such molecules are considered to have good potential to be major tools in the field of combinatorial chemistry.[66] Moreover, it is important for the field of molecular logic gates to have widespread application. Traditionally tagging in combinatorial chemistry has used mass spectrometric[67] and chromatographic[68] labels. Radiofrequency identification (RFID) chips have also been used to tag large containers of beads.[69, 70]

3.1.4 Literature Reviews of Molecular logic Gates

Grandini, P. et al[71] studied a lipophilic ligand, a fluorophore, and a surfactant which self-assemble in water to give a comicellar aggregation.[72] They selected the glycylglycine peptide, bearing a C_{10} linear alkyl chain at the N-terminus, as a ligand **18**. The 8-aniline-1-naphthalenesulfonic acid (ANS), and cetyltrimethylammonium bromide were used as the fluorophore and surfactant, respectively. The proximity between the

ligand and the fluorophore inside this aggregate should ensure contact between the complexed metal ion and the dye.This peptide is used to coordinate Cu(II) ion by means of its amino group, the deprotonated amido nitrogen atom and the carboxylate group.

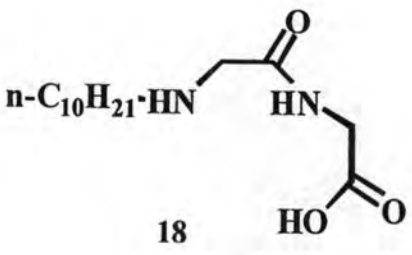

18

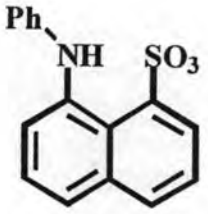

ANS

Nakahara et. al[73] examined the design and synthesis of monoazacryptand-type fluorophore chemosensor, **19** (derived from an 18-crown-6) and **20** (derived from a 15-crown-5) and their fluorescence properties for alkali metal and alkaline earth metal cation by using nonionic surfactants and ionic surfactants. The fluorescence of monoazacryptands is based on its pyrene ring, and is quenched due to PET from the amino nitrogen atom in the free state. Upon complexation with a metal cation, the nitrogen lone pair no long participates in PET, causing a recovery of the fluorescence. It was found that **19** showed highly selective Ba^{2+} due to only a small excess of Ba^{2+} to the ligand dramatically increased the fluorescence intensity of **19** in the presence of Triton X-100. The case of **20** detected alkaline earth metal cations more effectively than alkali metal cation in aqueous micellar solutions of anionic surfactants due to an enhancement of the electrostatic interaction between the anionic surfactants and alkaline earth metal cations, which have a large charge density. Therefore, **20** was used to detect K^+ in aqueous micellar solution of Tween-60 and showed specific Ca^{2+} and Mg^{2+} selectivity in aqueous micellar solutions of SDBS and TMADS, respectively.

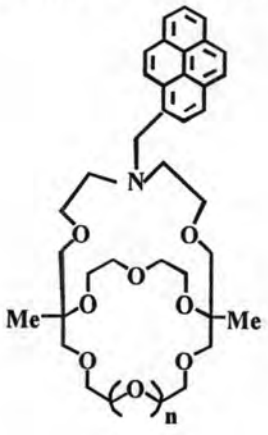

19 (n=1)
20 (n=0)

Pallavicini, P. et al.[74] designed and studied three tetrathia-monoaza macrocyclic ligand which have been synthesized with the same ring but functionalised on the nitrogen atom with methyl (**C1-NS4**), a *n*-butyl (**C4-NS4**) or a *n*-dodecyl (**C12-NS4**) chain. The three ligands have been in water containing TritonX-100 surfactants and pyrene used as fluorophore. The lipophilic **C12-NS4** has been developed as an ON-OFF fluorescence sensor for mecury. In the absence of Hg^{2+} at pH<4, the ligand is inside the surfactants, protonated and non-quenching, while on addition of mercury, the $[\mathbf{C12\text{-}NS4Hg}]^{2+}$ complex remains inside the surfactant and is quenching. On the other hand, the ligand of intermediate chain length, C4-NS4, can be used to obtain an OFF-ON sensor at pH 7.0-9.5 in the formation of $[\mathbf{C4\text{-}NS4Hg}]^{2+}$, which is hydrophilic to leave the surfactant and to be released from solution so it is no longer capable of quenching pyrene fluorescence.

C1-NS4

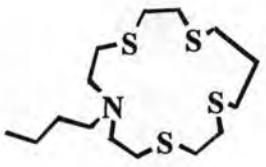

C4-NS4

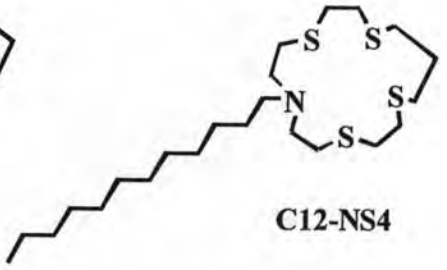

C12-NS4

Wang, P. et al.[75] synthesized several 1,5 –diphenyl-3-(2-pyridyl)-2-pyrazoline derivatives **21w-z** and investigated their complexation properties with divalent transition metal ions, Co^{2+}, Ni^{2+}, Cu^{2+} and Zn^{2+}. It was found that the addition of metal ions causes a decrease in intensity of the absorption maximum, which may correspond to the π-π^* transition, expect for Cu^{2+} ion. In this case, a new absorption band appears. These results indicate that derivatives **21w-z** have high binding affinity with metal ions. And these changes in the spectra present to estimate the stability constants and stoichimetries of the metal complexes. In the case for **21y**, the electron-withdrawing group (CN) on the 5-phenyl group decreases the quantum yield of **21y**. On complexation between Zn^{2+} and **21y**, this electron transfer effect may be relieved by the increased charge transfer from the 1-phenyl to the 3-pyridyl group. Consequently, the quantum yield of the complex is high. This makes it possible to detect the emission from the Zn^{2+} complex.

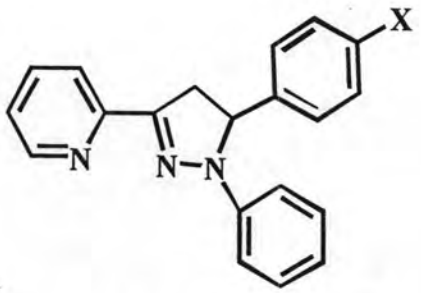

21w: X = H, 21x: X = OCH_3
21y: X = CN, 21z: X = NO_2

de Silva, A.P. et al.[76] synthesized 1,3-diaryl-Δ^2-pyrazoline which is flurophore-receptor system and used to be NOR molecular logic gate. The complexation can occur at 2, 2',6',2''-terpyridyl with H^+ or Hg^{2+}. Upon adding of H^+ or Hg^{2+}, the fluorescence output of **22** is quenched, this is obeyed by the NOR truth table.

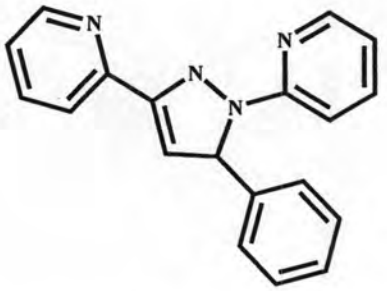

22

Moreover, the mechanism of fluorescence quenching with Hg^{2+} is possible to involve a nonemissive ligand-to-metal charge transfer (LMCT) excited state. In the case of H^+, it is easily understandable because the lone electron pair on N-2 interacts with hydrogen center.

3.1.5. Target Molecules

From the literature reviews, we have developed molecular logic gates in surfactants by using the self-assembled system created by hydrophobic receptors and fluorophores within the surfactant by synthesing the Na^+(**8b**) and Ca^{2+}(**10b**) receptors to use in the surfactant. Moreover, we synthesized several new pyrazolines **12b**, **13b**, **15b**, **16b**, **18b** and **20b** for use as fluorescent sensors and switches responding to protons for eventual use on bead surfaces were shown in Figure 3.1.

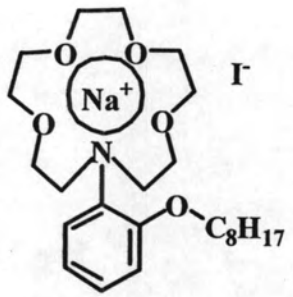

8b

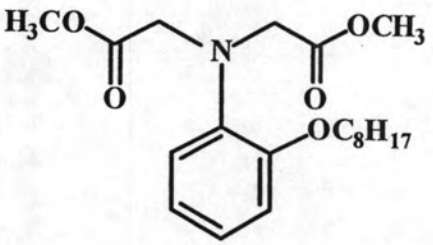

9b

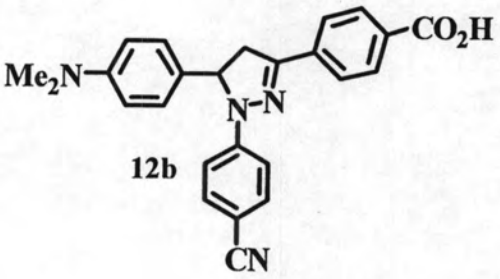

12b

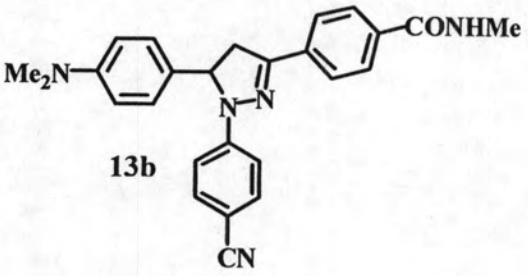

13b

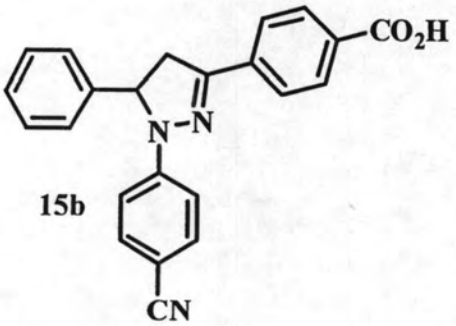

15b

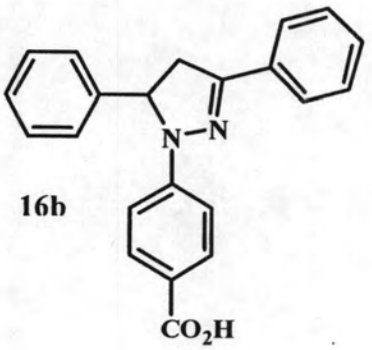

16b

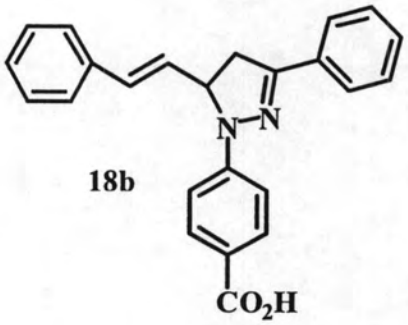

18b

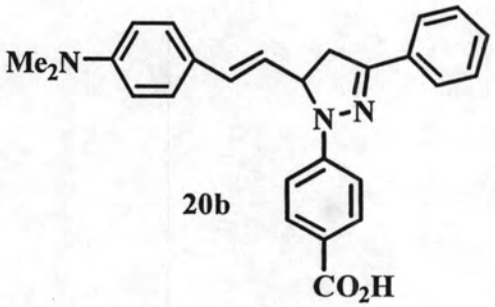

20b

Figure 3.1 Target molecules **12b**, **13b**, **15b**, **16b**, **18b** and **20b**

3.2 Experimental section

3.2.1 General procedure

3.2.1.1 Analytical instruments

Nuclear magnetic resonance (NMR) spectra were recorded in DMSO-d_6, $CDCl_3$ and CD_3CN on Varian 400 MHz spectrometer. Electrospray mass specta were determined on a Micromass Platform quadupole mass analyser with an electrospray ion source using acetonitrile as solvent. All melting points were obtained on an Electrothermal 9100 apparatus and uncorrected. Infrared spectra were carried out on a Nicolet Impact 410 FTIR spectrometer at room temperature with the potassium bromide (KBr) disk method. The sample was scanned over a range of 500-4000 cm^{-1} at resolution of 16 cm^{-1} and the number of scan was 32. The measurement was controlled by Omnic software. Absorption spectra were measured by a Varian Cary 50 UV-Vis spectrophotometer. Fluorescence spectra were performed on Varian Cary Eclipse spectrofluorometer by personal computer data processing unit. The light source is a pulse xenon lamp and a detector is a photomultiplier tube.

3.2.2 Synthesis of Receptor for H^+, Na^+ and Ca^{2+} in surfactant.

3.2.2.1 Preparation of *N*, *N*-bis(2-Hydroxylethyl)-2-methoxyaniline (2b)

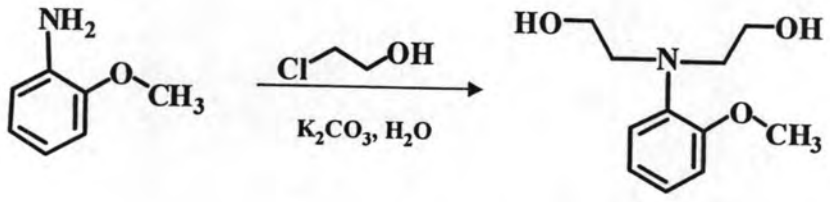

1b **2b**

A solution of **1b** (9.20 g, 81.00 mmol) in 2-chloro-ethanol (33 mL, 487 mmol) and water (88 mL) was heated to 80 °C for 15 min. K_2CO_3 (22.44 g, 160.00 mmol) was slowly added such that the temperature of this exothermic reaction was kept below 110 °C. The mixture was heated at 95 °C for 24 h, the reaction was cooled and 2-chloroethanol was removed under vacuum. The residue was diluted with water and extracted with $CHCl_3$. The $CHCl_3$ solution was dried over Na_2SO_4, and the solvent was evaporated, then purified by column chromatography using ethylacetate as eluent affording brown oil in (7.56 g, 70 % yield yield).

Characterization data for 2b

^{1}H-NMR Spectrum (300 MHz, $CDCl_3$): δ (ppm)

δ = 3.18 (t, 4H, NC*H*$_2$), 3.50 (t, 4H, OC*H*$_2$), 3.82 (s, 3H, ArOC*H*$_3$), 6.90-7.19 (m, 4H, Ar*H*)

3.2.2.2 Preparation of 2-Methoxyphenyl-15-crown-5 (3b)

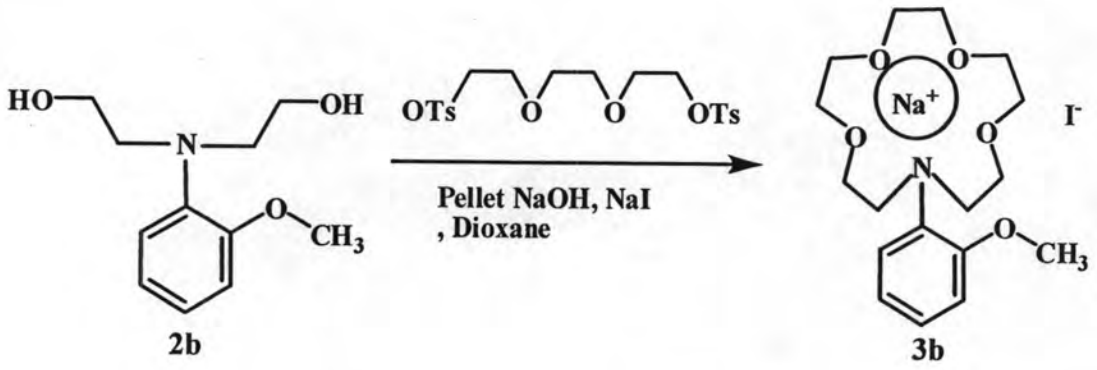

Compound **2b** (2.00 g, 9.48 mmol) was dissolved in dioxane (40 mL) and heated at 80 °C for 20 min. Pelleted NaOH (0.76 g, 18.90 mmol) was added slowly within about 3h. The temperature was then increased to 95 °C and tri(ethylene glycol)di-p-tosylate (1.77 g, 9.48 mmol) was added in one portion. The mixture was kept at 95 °C for 30 h. The suspension was then filtered hot, and the solvent was evaporated. The residue was treated with a solution of NaI (1.42 g, 9.48 mmol) in methanol (15 mL). The mixture was stirred at 60 °C for 30 min and ethyl acetate (20 mL) was added. The reaction was stirred at room temperature for 20 min, then allowed to stand at room temperature for 2 h. The resultant precipitate was filtered, washed with ethyl acetate, and dried at room temperature for 30 min to give azacrown-sodium iodide complex **3** as a soft yellow solid (0.05 g, 18% yield).

Characterization data for 3b

^{1}H-NMR Spectrum (300 MHz, $CDCl_3$): δ (ppm)

δ = 6.80-7.12 (m, 4H, Ar*H*), 3.98 (s, 3H, -OC*H*$_3$), 3.64 (m, 20H, -OC*H*$_2$)

ESI –TOF mass spectrum : $C_{17}H_{27}NO_5NaI$ = 348.1777 ([M+H$^+$]) m/z

3.2.2.3 Preparation of 1-nitro-2-(octyloxy)benzene (5b)

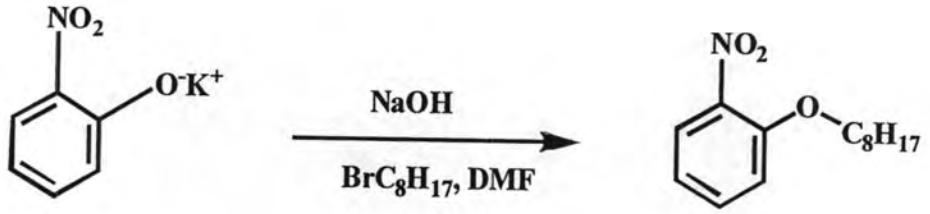

4b **5b**

Potassium 2-nitrophenoxide (26.80 g, 151.40 mmol), 1-bromooctane (27.55 g, 142.70 mmol) and N, N-dimethylformamide (DMF, 100mL) were heated to 130°C for 15 min. After cooling to room temperature, the precipitate (KBr) was filtered off and washed with 50 mL of 10% yield sodium hydroxide (precipitate dissolves in NaOH solution) and dichloromethane (50 mL). The combined organic phases were then further diluted with CH_2Cl_2, washed with 10% yield sodium hydroxide solution until no more orange colour appeared in the aqueous layer. The organic portion was then dried using anhydrous magnesium sulphate, filtered and concentrated under reduced pressure giving an orange liquid (20.16 g, 88% yield yield).

Characterization data for 5b

^{1}H-NMR Spectrum (300 MHz, $CDCl_3$): δ (ppm)

δ = 7.80(m, 1H, Ar*H*), 7.50(m, 1H, Ar*H*), 7.02(m, 2H, Ar*H*), 4.09(t, 2H, -OC*H*$_2$CH$_2$ J=6.5Hz), 1.82(m, 2H, -OCH$_2$C*H*$_2$), 1.46(m, 2H, -CH$_2$C*H*$_2$), 1.29(d, 8H, -CH$_2$(C$_4$*H*$_8$)CH$_3$, J=8.3Hz), 0.88(t, 3H -O(C$_7$H$_{14}$)C*H*$_3$, J=6.7Hz).

ESI –TOF mass spectrum : $C_{14}H_{21}NO_3$ = 251 ([M^+]) m/z

3.2.2.4 Preparation of 2-(octyloxy)benzenamine (6b)

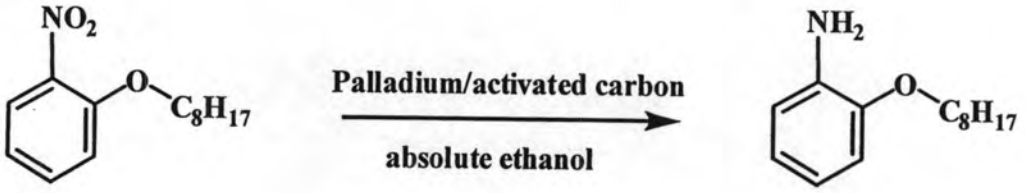

6b

Concentrated to yield a brown liquid **(5b)** (16.00 g, 72.30 mmol) was suspended in absolute ethanol, and Palladium (5% yield) on activated carbon (1.60 g, 10% by weight) was added. The system was evacuated and H_2 (g) was induced to a pressure of 30 psi (the pressure was checked every hour and refilled until no further change occurred). After stirred for 24 hours at room temperature, the reaction mixture was filtered and then dried over anhydrous $MgSO_4$, filtered and concentrated to yield a brown liquid (14.05 g, 82% yield).

Characterization data for 6b

^{1}H-NMR Spectrum (300 MHz, $CDCl_3$): δ (ppm)

δ = 6.80 (m, 4H, Ar*H*), 4.04 (t, 2H, -OC*H*$_2$CH$_2$), 3.88 (s, 2H, -ArN*H*), 1.88 (m, 2H, -OC*H*$_2$CH$_2$), 1.53 (m, 2H, -OCH$_2$C*H*$_2$CH$_2$), 1.39 (d, 8H, -CH$_2$(C$_4$*H*$_8$)CH$_3$,), 0.98 (t, 3H, -O(C$_7$H$_{14}$)C*H*$_3$).

3.2.2.5 Preparation of 2-(2-(octyloxy)phenylamino)diethanol (7b)

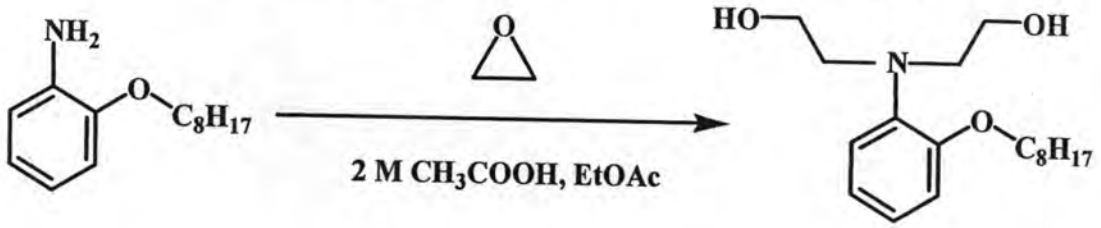

7b

In 3-necked flask, one neck was a pressure equalizing funnel. A mixture of **6b** (2.00 g, 9.04 mmol), 2M CH_3COOH (7.5 mL), Ethyl acetate (0.75 mL) was added to the pressure equalizing funnel. The weight of this entire assembly was recorded and then cooled to -30 °C using a dry ice/acetone mixture. Once at -30 °C the two stopper where removed and once was replaced by a bubbler and the other was connected to a bottle of ethylene oxide. Ethylene oxide was passed slowly through the apparatus until a sufficient amount had condensed in the round bottom flask. Both stoppers were replaced and the entire assembly (including the pressure equalizing tunnel) was weighted again to ensure enough ethylene oxide condensed. Once the correct amount of ethylene oxide had condensed. The reaction mixture (the presence equalizing funnel) was added drop wise to the condensed ethylene oxide and the flask was put back into the dry ice acetone bath and allowed to stir for 30 hours. Afterwards the two stoppers were removed and the reaction mixture was allowed to stir for a further hour. Na_2HCO_3 was added to neutralize the acid and the reaction mixture was extracted with dichloromethane (3 * 50 mL). The combined organic portion was dried with Na_2SO_4, filtered and concentrated at reduced pressure yielding brown oil (1.79 g, 90% yield).

Characterization data for 7b

^{1}H-NMR Spectrum (300 MHz, $CDCl_3$): δ (ppm)

δ=7.04 (m, 4H, Ar*H*), 3.98 (t, 2H, -OC*H*$_2$(CH$_2$)$_6$CH$_3$), 3.44 (t, 4H, -N(C*H*$_2$)$_2$OH), 3.18 (t, 4H, -N(C*H*$_2$)$_2$OH), 1.83 (m, 2H, -OCH$_2$(C*H*$_2$)$_6$CH$_3$)) , 1.36 (m, 10H, -OCH$_2$CH$_2$(C*H*$_2$)$_6$CH$_3$)), 0.87(t, 3H, -O(C$_7$H$_{14}$)C*H*$_3$)

3.2.2.6 Preparation of 2-Octoxyphenyl-15-crown-5 (8b)

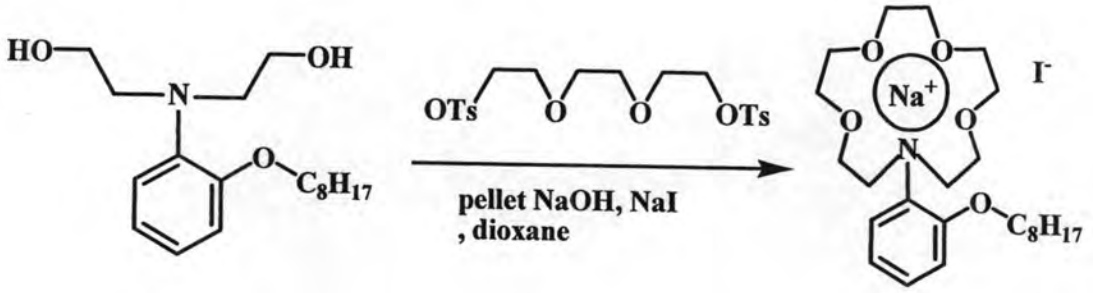

8b

Compound **7b** (3.00 g, 13.80 mol) was dissolved in dioxane and heated at 80 °C for 20 min. Pelleted NaOH (1.11 g, 27.00 mmol) was added slowly within about 3h. The temperature was then increase to 95 °C. Tri(ethylene glycol)di-*p*-tosylate (6.32 g, 13.80 mmol) was added in one portion, and the mixture was kept at 95 °C for 30 h. The hot suspension was then filtered. The solvent was evaporated, and the residue was treated with a solution of NaI in methanol. The mixture was stirred at 60 °C for 30 min and Ethyl acetate was added into the reaction which was kept stirring at room temperature for 20 min, then allowed to stand at room temperature for 2 h. The resultant precipitate was filtered, washed with ethyl acetate, and dried at room temperature for 30 min to give azacrown-sodium iodide complex as a soft yellow solid (0.85 g, 19.42% yield).

Characterization data for 8b

^{1}H-NMR Spectrum (300 MHz, $CDCl_3$): δ (ppm)

δ= 7.80 (m, 2H -Ar*H*), 7.1 (m, 1H, -Ar*H*), 6.94 (m, 1H, -Ar*H*), 3.17-4.16 (m, 22H, -O(CH_2)$_2$O- and –$OCH_2(CH_2)_6CH_3$), 1.80 (m, 2H, -$OCH_2(CH_2)_6CH_3$), 1.25 (m, 8H, -$OCH_2(CH_2)_6CH_3$), 0.88 (m, 3H, -$OCH_2(CH_2)_6CH_3$)

ESI –TOF mass spectrum : $C_{18}H_{41}NO_5Na$ = 446.2888 ([M+Na^+]) m/z

3.2.2.7 Preparation of *N*, *N*-di-(methylacetate)-2-(octyloxy) (9b)

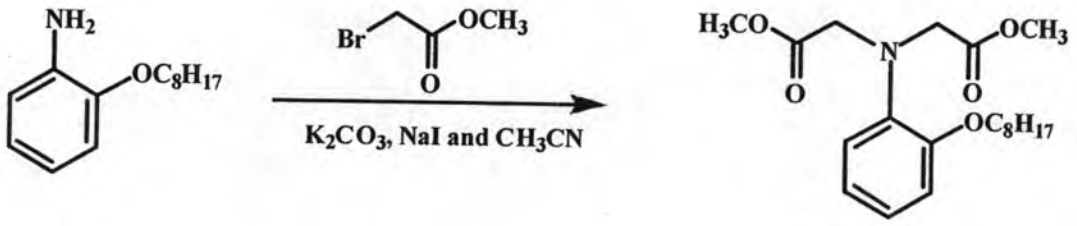

9b

2-(Octyloxy)aniline (2.00 g, 9.04 mmol), K_2CO_3 (2.50 g, 18.00 mmol), NaI (cat. amount) and methyl-2-bromoacetate (4.15 g, 27.10 mmol) were heated at 90°C in acetonitrile for 24 h. under N_2 atmosphere. Reaction mixture was cooled to room temperature. Acetonitrile (50 mL) was removed under reduced pressure. The remaining solid was partitioned between CH_2Cl_2 (3 * 50 mL) and water (3 * 50 mL). The aqueous partition was extracted with CH_2Cl_2 (1 * 50 mL) and the organic layer was dried with $MgSO_4$ and filtered to afford brown oil. The brown oil was purified by column chromatography using CH_2Cl_2: hexane = 1:1 and to provide as brown oil (1.39 g, 70% yield).

Characterization data for 9b

^{1}H-NMR Spectrum (300 MHz, $CDCl_3$): δ (ppm)

δ= 6.75-6.92 (m, 4H, -Ar*H*), 4.125 (s, -NCH_2-, 4H), 3.92 (t, -OCH_2-, 2H), 3.68(s, -OCH_3, 3H), 1.88 (m, -OCH_2CH_2, 2H), 1.53 (m, -OCH$_2$CH_2CH$_2$, 2H), 1.39 (d, -CH$_2$(C$_4H_8$)CH$_3$, 8H), 0.98 (t, -O(C$_7$H$_{14}$)CH_3, 3H).

ESI –TOF mass spectrum : $C_{18}H_{31}NO_5Na$ = 388.21 ([M+Na$^+$]) m/z

3.2.3 Synthesis of Receptor for H^+ and the effect of temperature on beads

3.2.3.1 Preparation of (*E*)-4-(3-(4-(dimethyamino)phenyl)acryloyl)benzoic acid (11b)

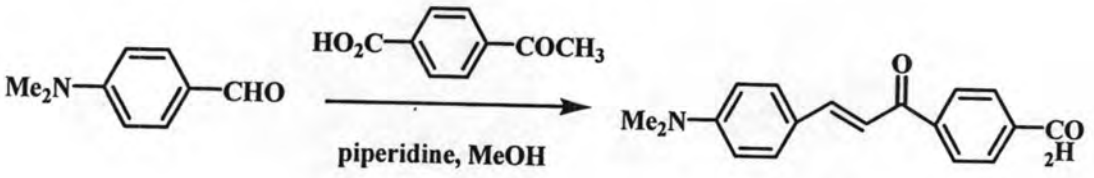

11b

The 4-(dimethylamino)benzaldehyde (2.72 g, 18.00 mmol), 4-acetylbenzoic acid (3.00 g, 164.10 mol) and piperidine (3.88 g, 45.0 mmol) were dissolved in dry methanol (HPLC grade) (10 mL). The solution was then refluxed at 90°C for 6 hours under N_2. The solution was cooled and refrigerated overnight. A dark red oil was deposited. This was separated and dried under vacuum. The precipitate was purified by crystallization using ethanol as solvent, yielding an orange crystal in (1.86 g, 85% yield).

Characterization data for 11b

^{1}H-NMR Spectrum (300 MHz, $CDCl_3$): δ (ppm)

8.18 (d, 2H, -Ar*H*, -C*H*N$(CH_3)_2$-)(J=8.5), 8.06 (d, 2H, -Ar*H*, -C*H*CO-)(J=8.16), 7.78 (d, 1H, -CH=C*H*-CO-)(J=15.1), 7.57 (m, 2H, -Ar*H*,-C*H*COOH-)(J=8.9), 7.33 (d, 1H, -C*H*=CH-CO-)(J=15.47), 6.68 (d, 2H, -Ar*H*, -C*H*-CH=CH)(J=8.53), 3.06 (s, 6H, -N$(CH_3)_2$).

ESI –TOF mass spectrum : $C_{18}H_{31}NO_5Na$ = 269 ([M+H^+]) m/z

IR Spectrum (KBr (cm^{-1})) : 2923, 2360, 1696, 1684, 1576, 1185, 1034, 982, 813, 730

Melting point: 178-179°C

3.2.3.2 Preparation of 4-(1-(4-cyanophenyl)-5-(4-(dimethylamino)phenyl)-4,5-dihydro-1*H*-pyrazol-3-yl)benzoic acid (12b)

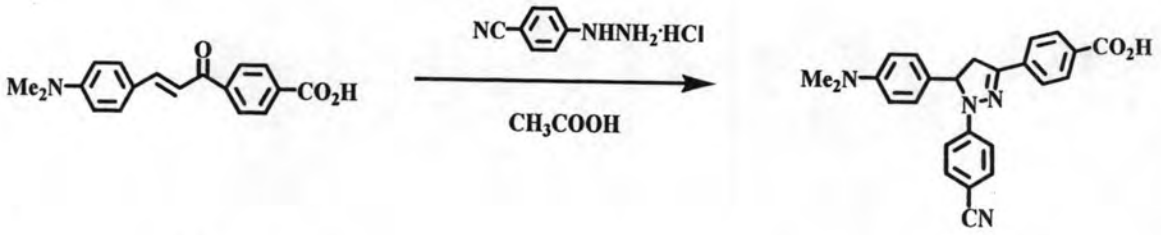

11b **12b**

A 1:1 ratio of **11b** (1.00 g, 3.39 mmol) and 4-cyanophenyl hydrazine hydrocholide (0.50, 3.39 mmol) was dissolved in boiling acetic acid (30mL) and left to stir for 3 hours. The mixture was then placed in the fridge overnight and a yellow crystal was obtained in (0.79 g, 80% yield).

Characterization data for 12b

^{1}H-NMR spectrum (300 MHz, $CDCl_3$): δ (ppm)

8.11 (d, 2H, -Ar*H*, -C*H*CN-)(J=8.26), 7.78 (d, 4H, -Ar*H*, -C*H*CHCN and –C*H*CN$(CH_3)_2$,)(J=8.5), 7.42 (dd, 4H, -Ar*H*, -C*H*COOH- and –C*H*-C-C)(J=20.32, 8.7.), 7.06(d, 2H, -Ar*H*, -C*H*CH), 5.50 (dd, 1H, -C*H*CH_2)(J=12.3, 5.68), 3.97 (dd, 1H, -CHCH_2-)(J=17.4, 12.4), 3.22 (dd, 1H, -CHCH_2-)(J=16.75, 5.44), 3.14 (s, 6H, -N(CH_3)$_2$).

ESI –TOF mass spectrum : $C_{25}H_{21}N_4O_2Ca$ = 452 ([M+Ca^{2+}+H^+]) m/z

IR spectrum (KBr (cm^{-1})) : 2922, 2628, 2213, 1700, 16011, 1546, 1397, 1099, 826, 774

Melting point: 236-237 °C.

3.2.3.3 Preparation of 4-[1-(4-Cyano-phenyl)-5-(4-dimethylamino-phenyl)-4, 5-dihydro-1H-pyrazol-3-yl]-N-methyl-benzamide (13b)

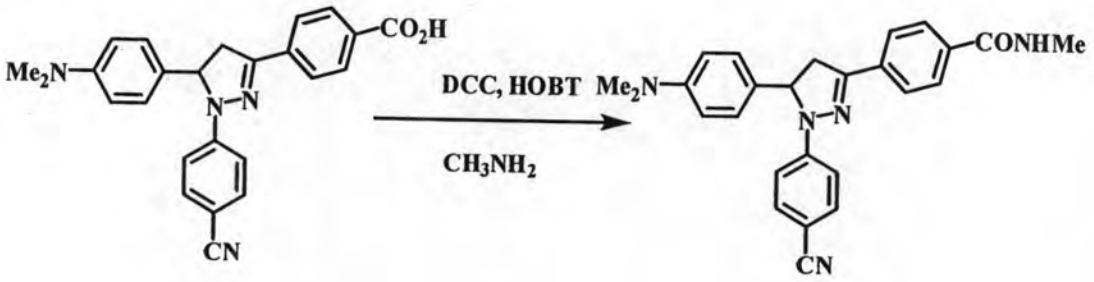

13b

4-(1-(4-Cyanophenyl)-5-(4-(dimethylamino)phenyl)-4,5-dihydro-1*H*-pyrazol-3-yl)benzoic acid (0.032 g, 0.077 mmol), DCC (0.019 g, 0.092 mmol), HOBT (0.012 g, 0.077 mmol) were dissolved in 20 mL CH_2Cl_2 (in a flask with a drying tube). Then the mixture was cooled to 0°C. CH_3NH_2 (0.0024 g, 0.077 mmol) was added into the reaction which was strirred at 0 °C for 1h. and the mixture was further stirred overnight at room temperature. The suspension was then filtered and the filtrate was evaporated. The residue was partitioned between ethyl acetate (15mL) and 5% yield $NaHCO_3$ aqueous solution (10mL). The ethyl acetate layer was washed with $NaHCO_3$ aqueous solution (2 * 10mL) and saturated NaCl aqueous solution (2 * 10mL). The ethyl acetate layer was then dried with anhydrous Na_2SO_4 and the solvent was evaporated to provide orange solid (0.028 g, 82% yield).

Characterization data for (13b)

^{1}H-NMR spectrum (300MHz, $CDCl_3$): δ (ppm)

8.87 (s, 4H, -Ar*H*, -C*H*CN and –C*H*CO-), 7.40 (d, 2H, -Ar*H*, -C*H*NMe_2), 7.07 (dd, 4H, -Ar*H*, -C*H*N-N and –C*H*-C-C=N-), 6.59 (d, 2H, -Ar*H*,-C*H*CN-), 6.14 (m, 1H, -CON*H*Me-), 5.30 (dd, 1H, -C*H*-CH_2), 3.86 (dd, 1H, -CH-CH_2), 3.18 (dd, 1H, -CHCH_2), 3.03 (m, 1H,-CONHCH_2).

ESI –TOF mass spectrum : $C_{26}H_{24}N_5O$ = 422 ([M-H^+])m/z

IR Spectrum (KBr (cm^{-1})): 3435, 3182, 3055, 3025, 2921, 2660, 1943

Melting point: 226-227°C.

3.2.3.4 Preparation of 4-cinnamoylbenzoic acid (14b)

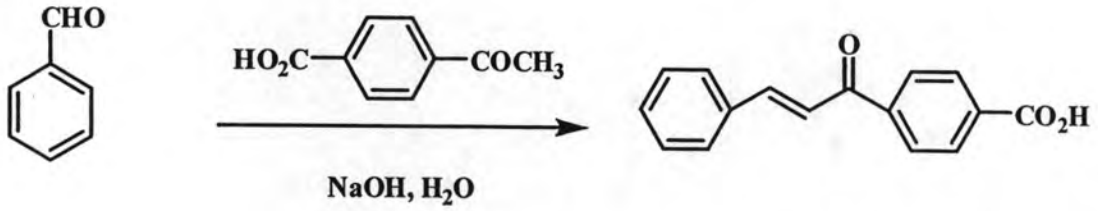

14b

Excess sodium hydroxide (0.84 g, 21.00 mmol) was dissolved in 100 mL water and 16 mL ethanol. Then a 1:1 ratio of 4-acetylbenzoic acid (3.44 g, 21.00 mmol) and benzaldehyde (2.14 g, 21.00 mmol) was added to the reaction mixture and left stirring at 35 °C for 5 h. The reaction mixture was then placed in a fridge overnight. The collected precipitate was purified by crystallization using acetic acid as solvent, yielding a yellow crystal (0.77 g, 85% yield).

Characterization data for (14b)

^{1}H-NMR spectrum (300 MHz, $CDCl_3$): δ (ppm)

8.23 (d, 2H, -Ar*H*, -COC*H*-)(J=8.53), 8.08 (d, 2H, -Ar*H*, -C*H*COO)(J=8.51), 7.86 (d, 1H -CH=C*H*-CO-)(J=15.4), 7.66 (m, 2H, -Ar*H*,-CHCH=CH-), 7.49 (d, 1H, -C*H*=CH-CO-)(J=15.76), 7.57 (m, 3H, -Ar*H*).

ESI –TOF mass spectrum : $C_{16}H_{12}O_3$ = 253 ([M+H$^+$]) m/z

IR spectrum (KBr (cm^{-1})): 3021, 2850, 2547, 1668, 1656, 1590, 1578, 1285, 1218, 946, 751

Melting point: 195-196°C.

3.2.3.5 Preparation of 4-(1-(4-cyanophenyl)-5-phenyl-4, 5-dihydro-1*H*–pyrazol-3-yl)benzoic acid (15b)

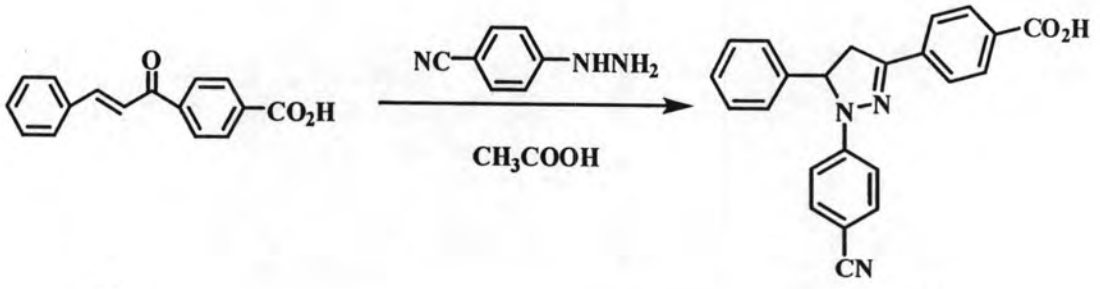

14b **15b**

A 1:1 ratio of **14b** (2.00 g, 0.79 mmol) and 4-cyanophenyl hydrazine (1.34 g, 0.79 mmol) was dissolved in boiling acetic acid (30 mL) and left to stir for 3 hours. The mixture was then placed in the fridge overnight and a yellow crystal was obtained (1.66 g, 84% yield).

Characterization data for 15b

^{1}H-NMR spectrum (300 MHz, $CDCl_3$): δ (ppm)

8.16 (d, 2H, -Ar*H*, -C*H*CN-)(J=8.34), 7.60 (d, 2H, -Ar*H*, -C*H*CHCN)(J=8.5), 7.39 (d, 2H, -C*H*COOH-)(J=8.91.), 7.32 (m, 5H, -Ar*H*), 7.28 (d, 2H, -Ar*H*,-CHCHCOO)(J=8.95), 5.30 (dd, 2H, -C*H*CH_2)(J=12.24, 5.96), 3.94 (dd, 1H, -CHCH_2-)(J=17.39, 12.37), 3.26 (dd, 1H, -CHCH_2-)(J=17.39, 5.97).

ESI –TOF mass spectrum : $C_{23}H_{16}N_3O_2$ = 368 ($M+H^+$]) m/z

IR spectrum (KBr (cm^{-1})) : 3022, 2923, 2215, 1693, 1603, 1510, 1292, 1178, 1101, 826, 699

Melting point: 248-249°C.

3.2.3.6 Preparation of 4-(3, 5-Diphenyl-4, 5-dihydro-pyrazol-1-yl)-benzoic acid (16b)

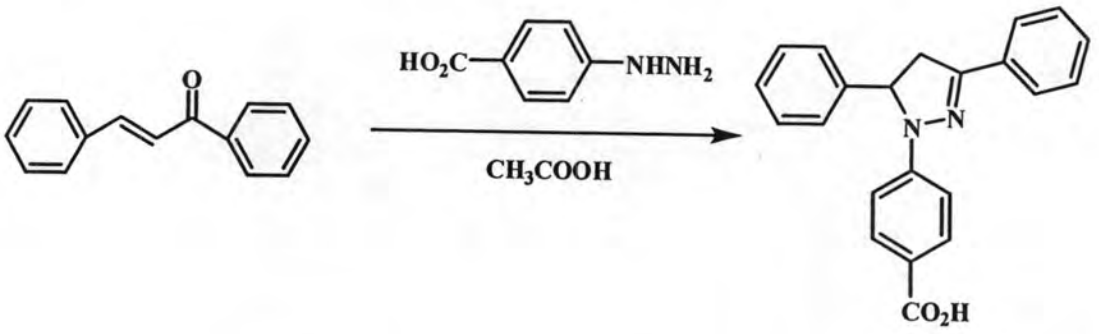

16b

A 1:1 ratio of chalcone (2.00 g, 9.60 mmol) and 4-hydrazinylbenzoic acid (1.46 g, 9.60 mmol) was dissolved in boiling acetic acid (30 mL) and left to stir for 3 h. The mixture was then placed in the fridge overnight and a yellow crystal was obtained. The collected precipitate was purified by crystallization using ethanol as solvent, yielding a yellow crystal (1.76 g, 85% yield).

Characterization data for 16b

^{1}H-NMR spectrum (300 MHz, $CDCl_3$): δ (ppm)

7.78 (d, 2H, -Ar*H*, CHCOOH)(J=6.1), 7.43 (d, 2H, -Ar*H*, -CHCN)(J=5.3), 7.35(m, 8H, -Ar*H*), 7.02 (d, 2H, -Ar*H*, -CHCHN)(J=13.78), 5.40 (dd, 2H, -C*H*CH_2) (J=6.02, 2.17), 3.91 (dd, 1H, -CHC*H*$_2$-) (J=17.0,9.85) , 3.21 (dd, 1H, -CHC*H*$_2$-) (J=7.71, 3.83).

ESI –TOF mass spectrum : $C_{22}H_{15}N_2O_2$ = 342.1322 ($M+H^+$]) m/z

IR Spectrum (KBr (cm^{-1})) : 3290, 3069, 3022, 2864, 2660, 2526, 2077, 1943, 1883, 1809

Melting point: 235-236 °C.

3.2.3.7 Preparation of (2*E*, 4*E*)-1, 5-diphenylpenta-2, 4-dien-1-one (17b)

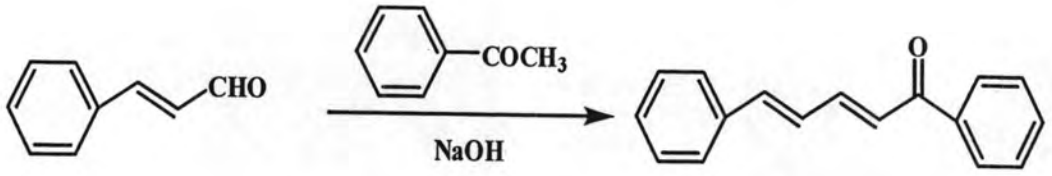

17b

Excess sodium hydroxide (4.62 g, 35.0 mmol) was dissolved in 100 mL water and 16 mL ethanol. Then a 1:1 ratio of acetophenone (4.20 g, 35.00 mmol) and cinnamaldehyde (4.62 g, 35.00 mmol) was added to the reaction mixture and left to stir at 35 °C for 5 hours. The reaction mixture was then placed in a fridge overnight. The collected precipitate was purified by crystallization using water and ethanol as solvent, producing a yellow crystal(3.53 g, 85% yield).

Characterization data for 17b

^{1}H-NMR spectrum (300 MHz, $CDCl_3$): δ (ppm)

8.04 (d, 2H, -Ar*H*, -COCH-) (J=8.31), 7.55 (m, 9H, -Ar*H*, and –C*H*=C*H*-CH), 7.32 (m, 3H, -Ar*H*).

ESI –TOF mass spectrum : $C_{17}H_4O$ = 235 ([M+H$^+$]) m/z

IR spectrum (KBr (cm^{-1})) : 3063, 3023, 2360, 1653, 1590, 1353, 1246, 777, 695

Melting point: 97-98°C.

3.2.3.8 Preparation of (*E*)-4-(3-phenyl-5-styryl-4,5-dihydropyrazol-1-yl)benzoic acid (18b)

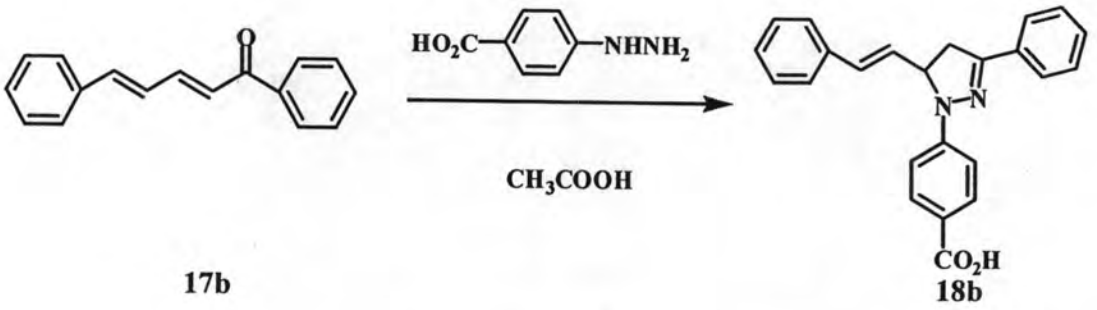

17b **18b**

A 1:1 ratio of **17b** (2.00 g, 8.54 mol) and 4-hydrazinylbenzoic acid (1.30 g, 8.54 mol) was dissolved in boiling acetic acid (30 mL) and left to stir for 3 h. The mixture was then evaporated and purified by column chromatography using 1:1 ethyl acetate and dichloromethane to provide a yellow crystal (1.79 g, 85% yield).

Characterization data for 18b

^{1}H-NMR spectrum (300 MHz, $CDCl_3$): δ (ppm)

7.96 (d, 2H, -Ar*H*, -CHCN-)(J=8.88), 7.77(d, 2H, -Ar*H*, -CHCOOH)(J=8.4), 7.33(m, 10H ,-Ar*H*), 6.62(d, 1H, -C*H*=CHCH-)(J=16.09), 6.22 (dd, 1H,-CH=C*H*CH-)(J=15.93, 7.4), 5.07 (dd, 1H, -CH=CHC*H*CH_2-)(J=12.48, 6.74), 3.71 (dd, 1H, -CH=CHCHCH_2-)(J=17.66, 12.12), 3.22 (dd, 1H, -CH=CHCHCH_2-)(J=17.13, 5.36).

ESI –TOF mass spectrum : $C_{24}H_{19}N_2O_2$ = 369 ([M+H^+]) m/z

IR spectrum (KBr (cm^{-1})) : 3025, 2531, 2360, 1671, 1596, 1591, 1430, 1284, 1088, 770, 690

Melting point: 158-160 °C.

3.2.3.9 Preparation of (2*E*, 4*E*)-5-(4-(dimethylamino)phenyl-1-phenylpenta-2,4-dien-1-one (19b)

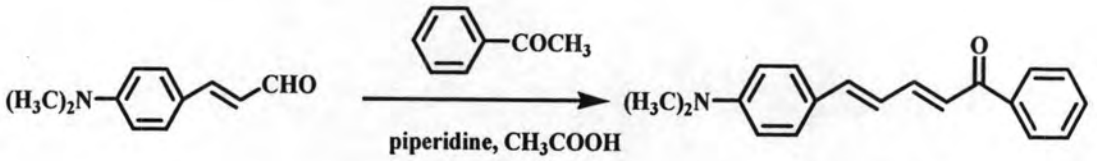

19b

The (E)-3-(4-(dimethylamino)phenyl) acrylaldehyde (4.00 g, 23.00 mmol) and acetophenone (2.74 g, 23.00 mmol) and piperidine (4.86 g, 57.00 mmol) were dissolved in 150 mL dry methanol (HPLC grade). The solution was then refluxed at 90°C for 6 hours under N_2 atmosphere. The solution was cooled and refrigerated overnight. A dark red oil was deposited, this was separated and dried under vacuum. The precipitate was purified by crystallization using ethanol as solvent, yielding a yellow crystal (2.63 g, 90% yield).

Characterization data for 19b

^{1}H-NMR spectrum (300 MHz, $CDCl_3$): δ (ppm)

7.95 (d, 2H, -Ar*H*, -C*H*N$(CH_3)_2$)(J=8.27), 7.59 (m, 6H, -Ar*H*, -C*H*-CO- and –C*H*=C*H*-), 6.94 (m, 3H, -Ar*H*), 6.70 (d, 2H, -Ar*H*, -C*H*-C-C*H*)(J=8.99), 3.02 (s, 6H, -N(CH_3)$_2$).

ESI –TOF mass spectrum : $C_{19}H_{19}NO$ = 278 ($M+H^+$]) m/z

IR spectrum (KBr(cm^{-1})) : 2923, 2360, 2341, 1557, 1355, 1283, 1007, 814, 668.

Melting point : 159-160°C

3.3.3.10 Preparation of (*E*)-4-(5-(4-(dimethylamino)styryl)-3-phenyl-4,5-dihydropyrazol-1-yl)benzoic acid (20b)

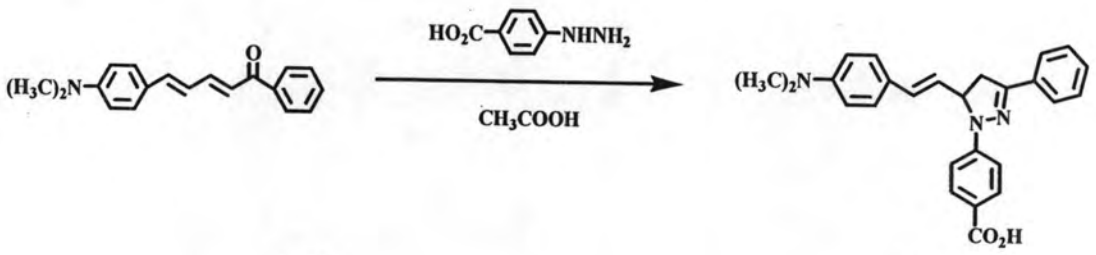

19b **20b**

A 1:1 ratio of **19b** (2.00 g, 7.22 mol) and 4-hydrazinylbenzoic acid (1.09 g, 7.22 mol) was dissolved in boiling acetic acid (30 mL) and left to stir for 3 h. The solution was evaporated and purified by column chromatography using 1:1 ethyl acetate and dichloromethane. A yellow crystal was obtained (1.79 g, 80% yield).

Characterization data for 20b

^{1}H-NMR spectrum (300 MHz, $CDCl_3$): δ (ppm)

8.06(m, 5H, -Ar*H*), 7.86 (d, 1H, -Ar*H*)(J=9.23), 7.44(m, 5H, -Ar*H* and –C*H*=CH), 7.17 (d, 2H, -Ar*H*)(J=6.5), 6.99 (d, 2H, -Ar*H*)(J=5.11), 4.38 (dd, 1H, -CH=CHC*H*CH_2-)(J=11.25, 11.13), 3.45 (dd, 1H, -CH=CHCHCH_2-)(J=10.83, 8.33), 3.03 (dd, 1H, -CH=CHCHCH_2-)(J=11.3, 8.3), 2.92 (s, 6H, -N(CH_3)$_2$).

ESI –TOF mass spectrum : $C_{26}H_{14}N_3O_2$ = 412.2008. (M+H$^+$]) m/z

Melting point : 295-296°C.

3.2.3.11 Reaction for immobilization on aminopropylsilica (5% yield loading) to give bead 12b

To a 50 mL round bottom flask with a drying tube was added aminopropylsilica (0.50 g, 0.045 mmol amine/g of beads) in HPLC grade DMF (20 mL). The beads were then swollen for 10 min. under stirring. Then R-CO_2H (0.011 mmol), 1-hydroxybenzotriazole (HOBT) (0.017 g, 0.11 mmol), 1,3-dicyclohexyl carbodimide (DIC) (0.15 mL, 0.96 mmol) were added and the mixture was stirred for 3 hr. The beads were washed sequentially with DMF (2 * 20 mL portion), DMF:MeOH (1:1) (2 * 20mL portions) and MeOH (2 * 20 mL portions) and then allowed to dry.

3.2.4 Fluorescence studies

3.2.4.1 For surfactant

A small amount of CH_3OH (<1% yield, v/v) was used to facilitate the solubility of fluorophores such as hydrophobic tris(bipyridine)Ru(II), pyrene and 9-cyanoanthracene in the Triton X-100 or SLS surfactant solution. The absorbance of the fluorophore at a wavelength of maximum absorption in the final surfactant solution was approximately 0.1. This was chosen as the excitation wavelength for obtaining the fluorescence emission spectra. pH titrations were usually conducted from pH 2.0 to pH 10.0 using aliquots of NaOH and HCl. In the case of Na^+ and Ca^{2+}, concentrations of 0-1.0 M were used. In the case of Ca^{2+} experiments, the calcium-free condition was achieved by employing 10.010 mM EDTA. Equation (1.2) was employed to calculate pK_a values and log β values.

3.2.4.2 Bead studies and preliminary studies in homogeneous solution

The absorbance of the fluorophore at a wavelength of maximum absorption in the final surfactant solution was approximately 0.1. This was chosen as the excitation wavelength for obtaining the fluorescence emission spectra. The spectral properties of the compounds were investigated in a MeOH : H_2O (1:1, v/v) solution using aliquots of NaOH and H_3PO_4 to vary pH values usually from pH 2.0 to pH 10.0 pK_a Values were calculated by using equation (1.2).

3.3 Results and discussion

3.3.1 The results and discussion for molecular logic gates in surfactant

This research was concerned with the self-assembly of fluorophores and receptors within a detergent surfactant compartment so that the separation distance between the former pair will be sufficiently small that a PET process would occur. Since fluorophores are normally present in very low concentration, normal statistics would rule that many surfactant compartments will be devoid of fluorophores. What matters will be those surfactants which happen to have a resident fluorophore. Would a sufficiently fast PET process arise under these circumstances? Intramolecular versions of this system have produced fast PET rates, which in turn led to sensor/switch/logic systems which have received wide attention. Nevertheless, intramolecular versions require synthesis of relatively complicated structures. On the other hand, the self-assembly approach requires simpler compounds and also possesses the feature of flexibility. If one component does not function appropriately, it can easily be substituted with another. So, if successful, the self-assembly approach would lead to 'plug and play' molecular logic systems. This required functionalization of both the fluorophore and the receptors in order to anchor them in the surfactant structure. It has already been shown that the self-assembly of sensor systems is possible from the work carried out by Diaz-Fernandez et al.[77] This work planned to use a fluorophore with a long excited state lifetime in order to maximize the chances of a successful PET event occurring. Since tris(4,4'-bipyridyl)Ru(II) **(20)** possesses one of the longest lifetimes without a large amount of quenching in ambient aerated solutions, it was selected to be the fluorophore. However, as tris(4,4'-bipyridyl)Ru(II) can only be incorporated into anionic surfactant structures for electrostatic reasons it was felt that this limited its adaptability. Modifications were made so that we could use the fluorophore in combination with several surfactant types. In this work, a more hydrophobic fluorophore had to be synthesized, while the favourable optical properties were preserved. We chose bis(bipyridyl)-4,4'-dinonylbipyridylRu(II) ion **(24)** which has two nonyl chains to increase the hydrophobicity. Bis(bipyridyl)dichloroRu(II) **(22)** and 4,4'-dinonylbipyridine **(23)** were reacted as shown in scheme 3.2.

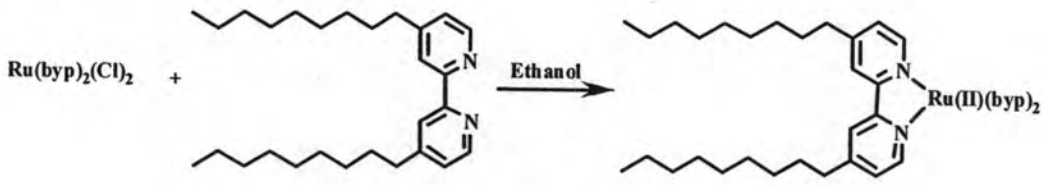

21 22 23

Scheme 3.1. Synthesis of bis(bipyridyl)-4,4′-dinonylbipyridylRu(II) **(23)**

24 25 26

Figure 3.2 Showing structure of tris(4,4'-bipyridyl)Ru(II) **(24)**, pyrene **(25)** and cyanoanthracene **(26)**

3.3.2 Preparation of the receptors

We also needed to prepare a receptor that would incorporate itself into the surfactant structure. This is necessary to allow a close association between the fluorophore and receptor within the surfactant leading to a successful PET interaction between them. A solution of **1b** in 2-chloroethanol and water was heated to 80 °C for 15 min. K_2CO_3 was slowly added such that the temperature of this exothermic reaction was kept below 110 °C. The mixture was heated at 95 °C for 24 h and cooled, 2-chloroethanol was removed under vacuum. Then, it was purified by column chromatography to afford brown oil. Compound **1b** changed to be compound **2b**, the ^{1}H-NMR showed the CH_2 of compound **2b** at 3.50 ppm. Compound **2b** was dissolved in dioxane and heated at 80 °C for 20 min. Pelleted NaOH was added slowly within about 3 h. The temperature was then increase to 95 °C. Tri(ethylene glycol)di-*p*-tosylate) was added in one portion, and the mixture was kept at 95 °C for 30 h. The suspension was then filtered hot and the solvent

was evaporated. The residue was treated with a solution of NaI in methanol. The mixture was stirred at 60 °C for 30 min and ethyl acetate was added and the mixture was stirred at room temperature for 20 min, and then allowed to stand at room temperature for 2 h. The resulting precipitate was filtered, washed with ethyl acetate, and dried at room temperature for 30 min to give azacrown-sodium iodide complex **3b** as a soft yellow solid. It was found that the [-CH_2-CH_2-O-] of compounds **3b** was at 3.64 ppm and the mass result of compound **3b** was shown m/z at 348.1777 of [$M+H^+$].

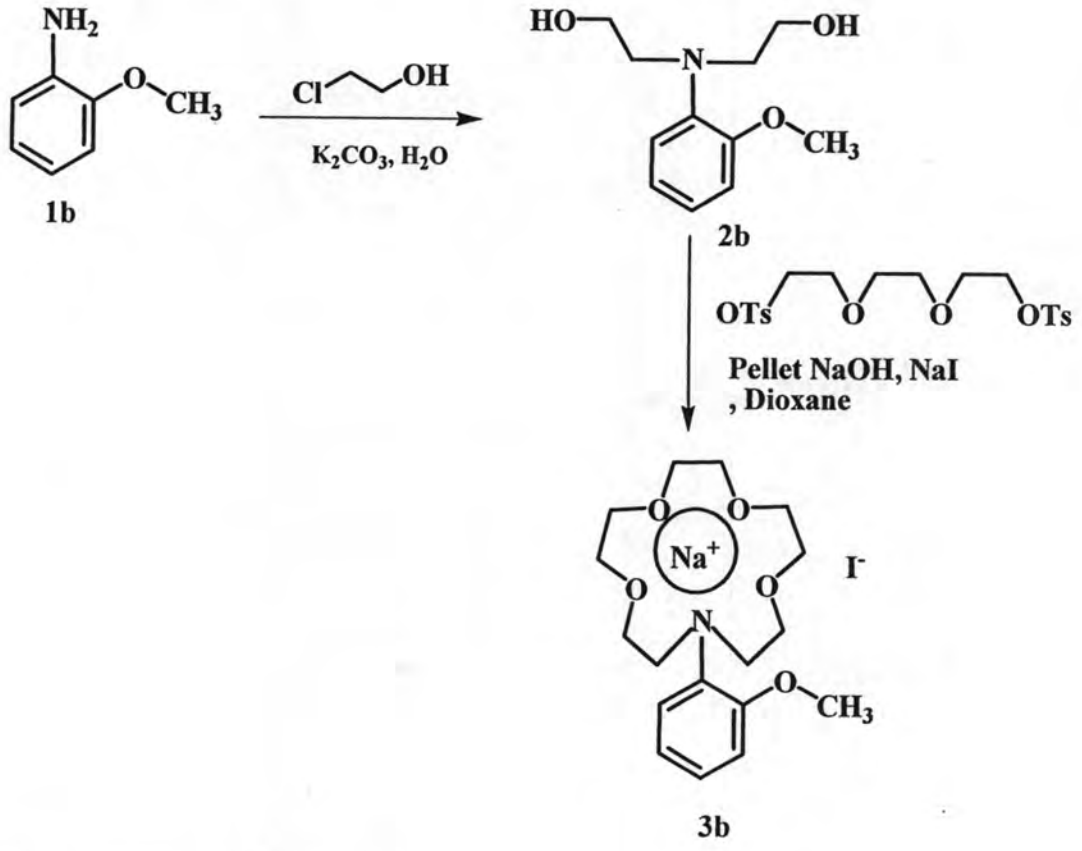

Scheme 3.2 Synthesis of 2-methoxyphenylaza-15-crown-5 ether (**3b**).

When the receptor **3b** was tested in fluorescence experiments, it was not found to be hydrophobic enough to locate in the surfactant for 'plug-and-play' action. Therefore we modified **3b** to increase its hydrophobicity by synthesizing sensor **8b** as shown in scheme 3.4. Thus, the molecular receptors should also be modified to carry a long alkyl chain. Receptor **6b** for H^+ was prepared as shown in Scheme 3.2.

The synthesis of the sodium receptor **8b** was started using potassium 2-nitrophenoxide **4b** and 1-bromooctane in DMF which were heated to 130°C for 15 min. After cooling to room temperature the precipitate (KBr) was filtered off and washed with 10% yield sodium hydroxide (50 mL) and CH_2Cl_2 (50 mL). The precipitate dissolves in NaOH solution. The CH_2Cl_2 layer was concentrated to yield a brown liquid. The brown liquid **8b** was found the peaks $-CH_2-$ and $-CH_3$ protons of $-OC_8H_{17}$ group at 4.09 (2H), 1.82(2H), 1.46 (2H), 1.29(8H) and 0.88(3H) ppm, the mass result was at 251[M^+]. Compound **5** was suspended in absolute ethanol and Palladium (5% yield) on activated carbon was added. The system was evacuated and H_2 (g) was introduced to a pressure of 30 psi. The pressure was checked every hour and refilled until no further change occurred. The reaction mixture was stirred for 24 hours at room temperature, filtered, dried over anhydrous $MgSO_4$ and evaporated affording brown oil **6b** which was observed at 3.88 ppm of [-ArN*H*-]. Methyl-2-bromoacetate was added to **6b** in acetonitrile and refluxed under N_2 with stirring for 24 hours at 90°C.

Then, the mixture of acetic acid, ethyl acetate and compound **6b** were added the condensed ethyleneoxide, the reaction was stirred overnight. The mixture was extracted by CH_2Cl_2 and the organic layer was evaporated to get brown oil. It was observed the peaks at 3.44 and 3.18 ppm [$-O(CH_2)_2OH-$] of compound **7b**. Compound **7b** was dissolved in dioxane and heated at 80 °C for 20 min. Pelleted NaOH was added slowly within about 3 h. The temperature was then increase to 95 °C. Tri(ethylene glycol)di-p-tosylate was added in one portion, and the mixture was kept at 95 °C for 30 h. The suspension was then filtered hot and the solvent was evaporated. The residue was treated with a solution of NaI in methanol. The mixture was stirred at 60 °C for 30 min and ethyl acetate was added and the mixture was stirred at room temperature for 20 min, then allowed to stand at room temperature for 2 h. The resulting precipitate was filtered, washed with ethyl acetate, and dried at room temperature for 30 min to give azacrown-sodium iodide complex as a soft yellow solid. The yellow solid was shown mass at 446.2888 of [M+Na^+].

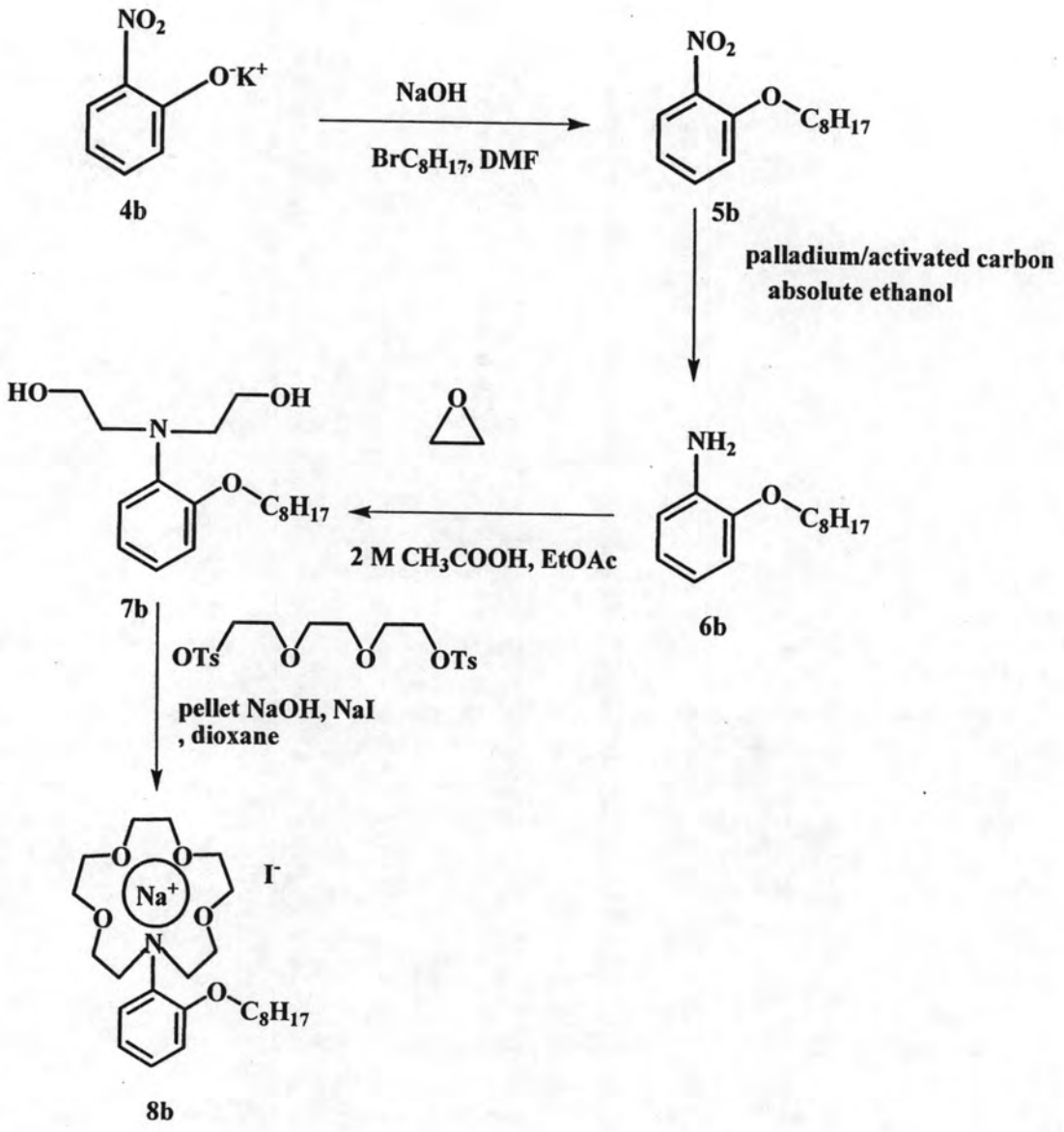

Scheme 3.3 Synthesis of 2-octyloxyphenyl-15-crown-5 ether (**8**b).

Scheme 3.4 Methyl-2-bromoacetate was added to **6** in acetonitrile and refluxed under N_2 with stirring for 24 hours at 90°C. The reaction mixture was cooled to room temperature and purified by column chromatography using DCM:hexane (1:1) as eluent. The methyl ester groups of **9** were hydrolysed with KOH in THF to give compound **10** as shown in Scheme 3.4. The $-CH_2-$ and $-CH_3$ methyl ester groups of compound **9** was shown at 3.92 and 3.68 ppm, respectively. The mass result was found at 388.21 of $[M+Na^+]$.

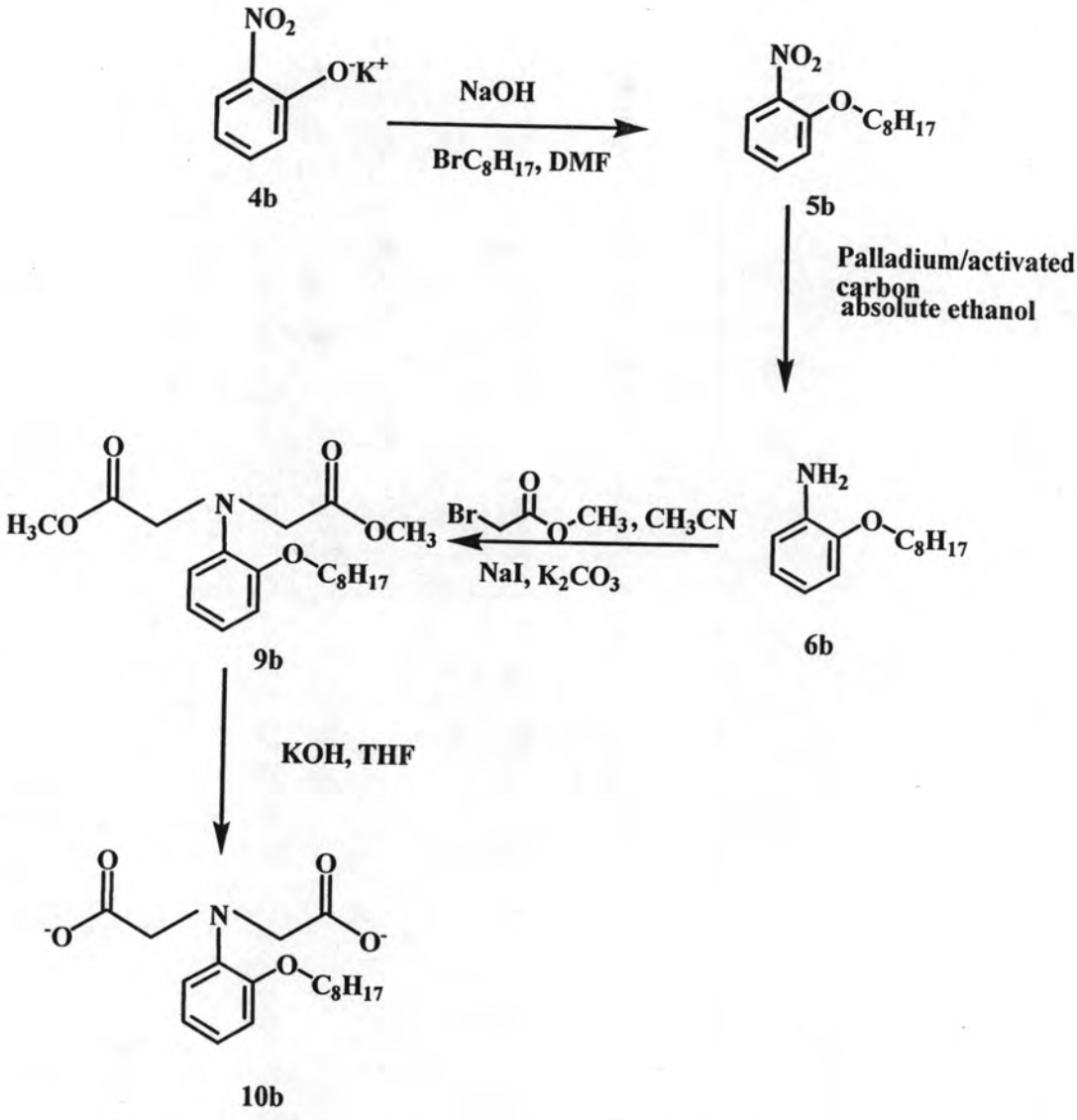

Scheme 3.4 Preparation of *N*,*N*-di-(methylacetate)-2-(octyloxy)

While two of the receptors used in this study were synthesized as described above, several other simpler cases were available for purchase. The purchased receptors were 4-tertbutylphenol **(27)**, 4-octylphenol **(28)**, 4-octylaniline **(29)**, 4-octylpyridine **(30)** and 4,4′-pyridine **(31)** as shown in Figure 3.1. It is noted that the deprotonated form of the phenols serve as the H^+ receptors.

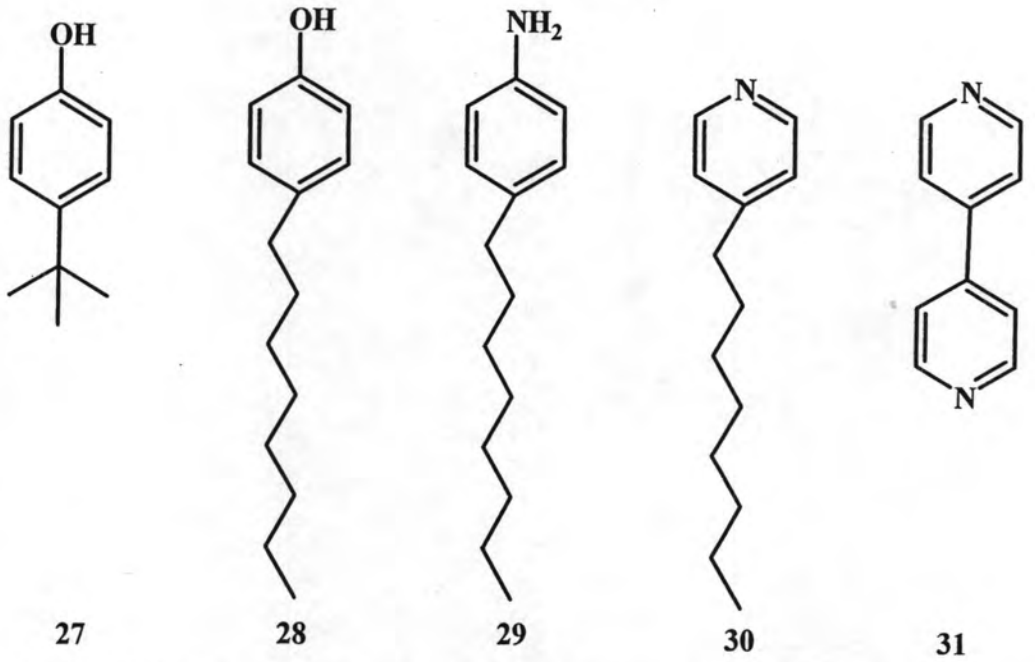

Figure 3.3 Structures a) 4-tertbutylphenol **(27)**, b) 4-octylphenol **(28)**, c) 4-octylaniline **(29)**, d) 4-octylpyridine **(30)** and e) 4,4'-bipyridine **(31)** used in this study

3.3.3 Surfactant

There are three types of surfactants. The first is a cationic surfactant such as CTAC (Cetyl Trimethyl Ammonium Chloride), the second is neutral such as Triton X-100 and the last one is anionic such as SLS (Sodium Lauryl Sulfate). The surfactant serves to assemble the fluorophore and receptor in close proximity and also serves as a spacer between them. In contrast, intramolecular examples of fluorescent sensors/switches contain a spacer covalently bound to the two key components. A number of combinations of surfactant, fluorophore and receptor were investigated.

3.3.4 The Fluorescence Studies for molecular logic gates in surfactant

3.3.4.1 Pass 0 logic gate

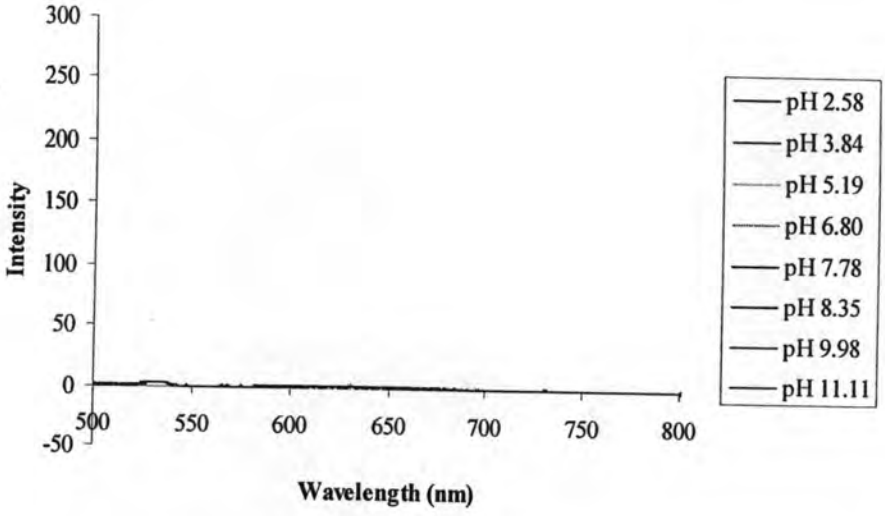

Figure 3.4 Fluorescence spectra of Triton X-100 solution as a function of pH (λ_{ex} = 450 nm, λ_{em} = 620 nm)

The initial system has only Triton X-100 as it is important to know that the surfactant solutions will provide a low and pH-independent background with respect to fluorescence output. This initial system also provides an example of an extremely simple logic gate, the PASS 0. When H^+ was considered as the input and fluorescence (excited at 450 nm and emitted at 620 nm) was taken as output, this means that the fluorescence remains nearly zero, i.e. remains in the 'off' state whether the pH is high or low.

3.3.4.2 Pass 1 logic gate

The output of the fluorophore should not be influenced by the analyte being investigated, H^+ in this case. Therefore it was also necessary to run titrations with only the fluorophore and the surfactant present. This is an example of another rather simple logic gate, the PASS 1 gate. The fluorescence output remains in the 'on' state as the pH is changed from a highly alkaline (pH 11) to a highly acidic (pH 2) environment.

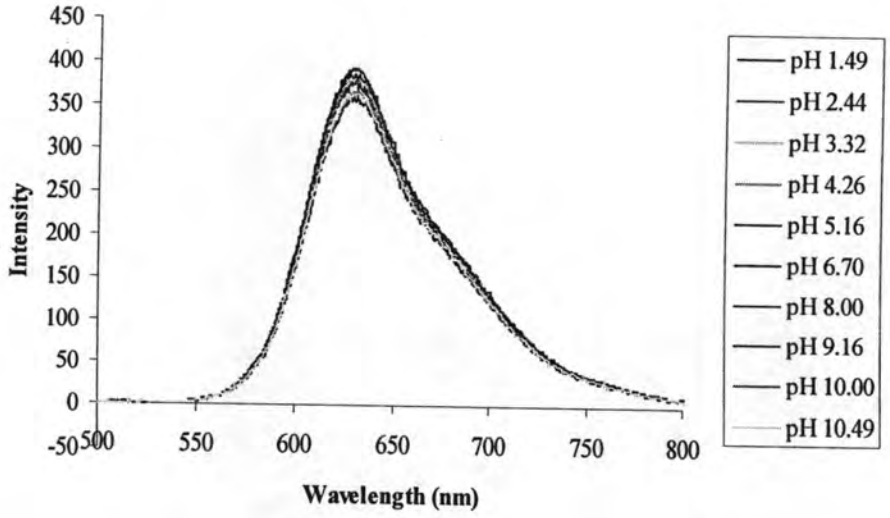

Figure 3.5 Fluorescence spectra of **21** in SLS solution as a function of pH (λ_{ex} = 450 nm, λ_{em} = 620 nm).

3.3.4.3 YES logic gate

The fluorescence-pH titrations were now extended to surfactant solutions containing both the fluorophore and the receptor so that we could start to examine our approach to assembling more complex logic gates.

3.3.4.3.1 H^+-driven gates using 4-octylaniline (29)

Knowing that the fluorescence output of the fluorophore in the presence of the surfactant will remain independent of the pH of the solution allows the testing of receptors for H^+ and other target species. The use of amines as receptors for protons is common. Long aliphatic chains are routinely used to allow molecules to be incorporated into surfactants, thus 4-octylaniline **(29)** should be able to act as a suitable surfactant-bound receptor for protons. It is known that the fluorescence of tris(bipyridyl)Ru(II) is quenched by anilines via PET in intermolecular situations[79] and also via other mechanisms in intramolecular situations[80]. When it is combined with the fluorophore and the surfactant solution a small response is seen when titrated over a range of pH values. Using a combination of SLS surfactant, as the fluorophore, and a fluorescence enhancement (FE) of 1.1 was found (Table 3.1) and shown in Figure 3.6. However, a

similar magnitude of fluorescence variation was seen in Figure 3.6 where the receptor was absent. In other words, the receptor **(29)** is not able to cause a significant PET rate to the fluorophore in the present case when the H^+ guest is absent. By changing the fluorophore to the more hydrophobic version **(23)** (while keeping the receptor and surfactant the same) a small decrease in the FE was observed to 1.1.

The FE values found in these experiments were far less than expected. The SLS surfactant was expected to hold the fluorophore and the receptor in close proximity. The current results suggest that the cationic fluorophore **(21** or **23)** is pinned to the sulfate headgroups of the SLS surfactants whereas the receptor appears to be localized some distance away, i.e. deeper towards the micellar core. In intramolecular cases, PET rates fall off sharply with increasing distance of separation e.g. 0.3 nm [81]. Since SLS surfactants have a radius of about 3 nm when the ion cloud is included[82], the fluorophore and receptor can occupy sites within an individual surfactant such that the PET rates are poor. Hence the H^+-induced stopping of PET and the subsequent FE value are low. Though the variation is small, the fluorescence intensity (I_F) as a function of pH can be analyzed according to a version of equation (1.2) mentioned in the introduction chapter. The pK_a value characterizes the H^+-binding strength of the receptor in its micellar environment. The pK_a values are 7.6 and 7.8 in the two cases involving the same receptor, with large associated uncertainties owing to the small FE values of 1.2 and 1.1 respectively.

By switching from SLS to the non-ionic Triton X-100, the situation was improved. The FE value rose to 2.9 for the hydrophobic fluorophore **23**. The parent fluorophore **21** is not hydrophobic enough to be anchored to the non-ionic surfactant, unlike the electrostatic binding seen in anionic SLS. So now we can reasonably describe the system as a H^+-driven YES logic gate. The pK_a value is 3.7. This can be compared with the value of 7.8 seen in SLS. Surfactants exert dielectric and electric effects on pK_a values [83, 84]. In the case of amine receptors, the H^+-binding is harder due to the lowered polarity of the surfactant (Triton X-100) compared to water. Hence the pK_a value is lowered compared to 5.1, the value for model compound 4-methylaniline in water [85]. Hence the observed pK_a value of 3.7 for the present case of 4-octylaniline **(29)** in Triton X-100 is understandable.

The protonated amine group is electrostatically stabilized by anionic surfactants such as SLS, and protons are concentrated at the micellar surface. This causes an apparent increase of amine basicity. Therefore a higher pK_a value can be expected. However, SLS

also has a lowered polarity which causes an opposite effect on pK_a values as described above. Nevertheless the net result is a raised pK_a value. Hence the observed value of 7.8 in SLS is sensible.

This is a sutiable moment to mention that cationic surfactants were not examined in this work since they repel H^+ from their surfaces, making the assembly of surfactant, fluorophore, receptor and H^+ much less likely.

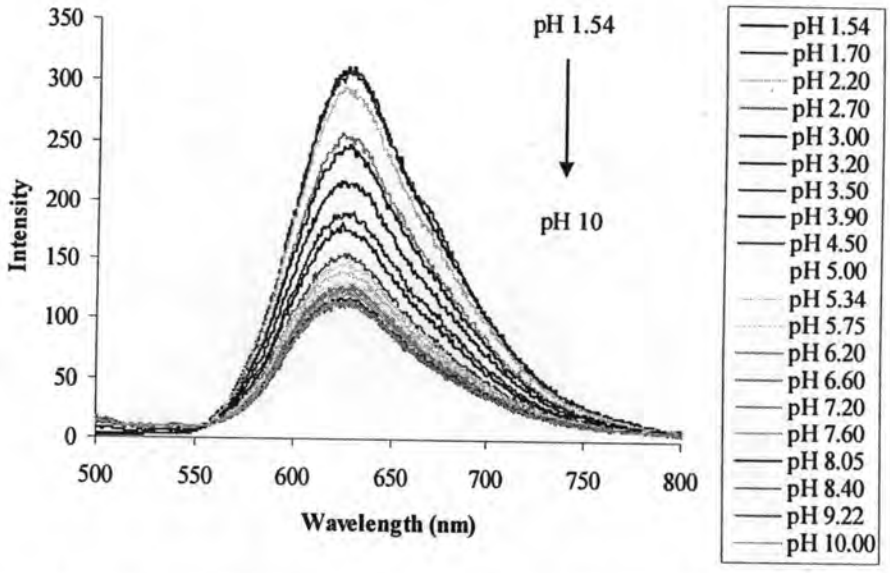

Figure 3.6 Fluorescence spectra of hydrophobic RuBpy **(23)** and 4-octylaniline **(29)** ($1 * 10^{-3}$ M) in SLS solution as a function of pH (λ_{ex} = 450 nm, λ_{em} = 620 nm)

Unlike 4-octylaniline **(29)** which is commercially available, 2-octyloxyaniline **(6)** had to be synthesized according to Scheme 3.4. 2-Octyloxyaniline **(6)** showed a similar pattern of action when compared to 4-octylaniline **(29)**, however the FE of the systems were slightly increased. For the SLS and 2-octyloxyaniline **(6)** system a FE value of 1.6 was obtained. A FE value of 1.2 was obtained when the more hydrophobic **23** was used in SLS suggesting that the increased distance from the fluorophore decreases the efficiency of PET, hence reducing the FE value. Once the surfactant medium was changed to Triton X-100 a large increase in the FE was observed again to 2.9. As with the case with 4-octylaniline the change in the FE is accompanied by a change in the pK_a of the receptor. This can be explained by the anionic headgroups of SLS concentrating H^+ near its surface. Hence the increase in the pK_a value in SLS (6.5) compared to that in Triton X-

100 (2.5). The corresponding value of a model receptor (2-methoxyaniline) in water is 4.5 [85] lies in-between these two values as explained above for the 4-octylaniline **(29)** case.

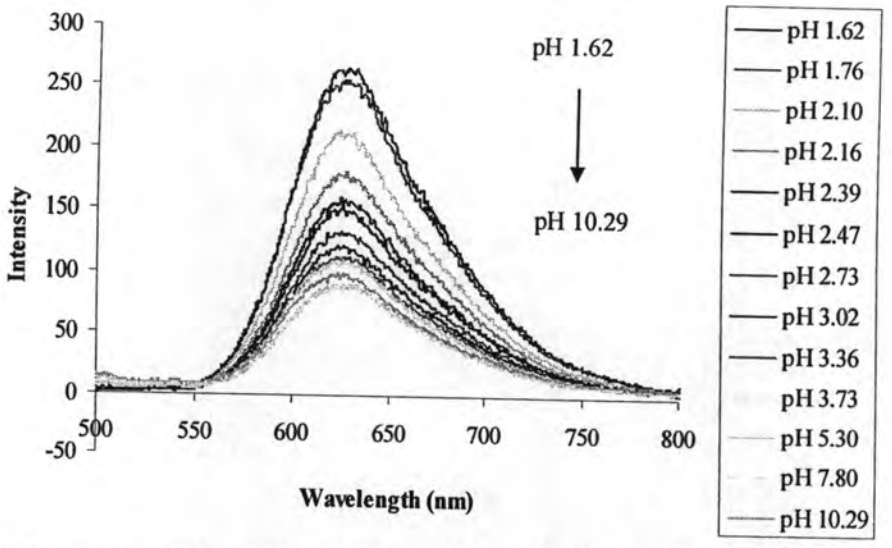

Figure 3.7 Fluorescence spectra of **23** and 4-octylaniline **(29)** ($1 * 10^{-3}$ M) in Triton X-100 solution as a function of pH (λ_{ex} = 450 nm, λ_{em} = 620 nm) (YES gate).

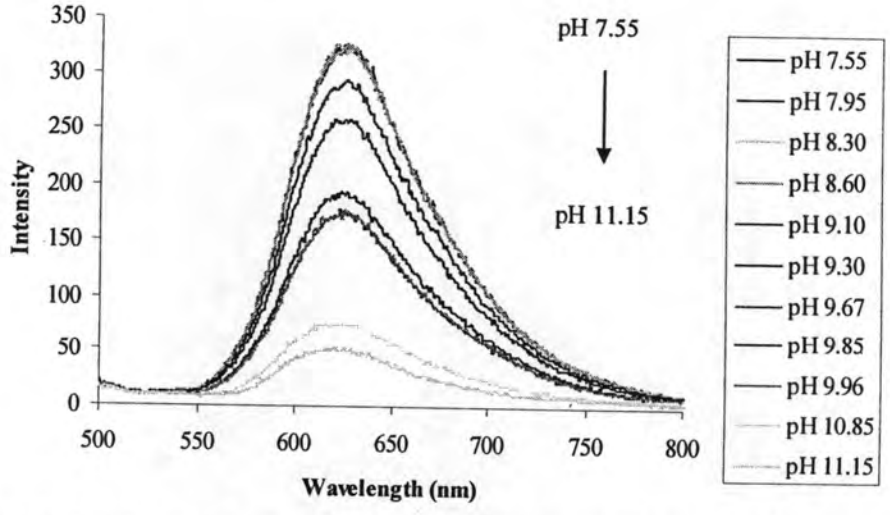

Figure 3.8 Fluorescence spectra of **23** and 4-octylphenol **(28)** ($1 * 10^{-3}$ M) in Triton X-100 solution as a function of pH (λ_{ex} = 450 nm, λ_{em} = 620 nm) (YES gate).

Table 3.1 pK_a and FE values of various surfactant, receptor and fluorophore assemblies.

Surfactant	Receptor	Fluorophore	pK_a	FE
SLS	**29**	**21**	7.60	1.18
SLS	**6**	**21**	6.70	1.57
SLS	**28**	**21**	12.20	1.45
SLS	**31**	**21**	4.60	1.45
SLS	**29**	**23**	7.80	1.07
SLS	**6**	**23**	6.50	1.19
SLS	**28**	**23**	12.20	1.30
Triton X-100	**29**	**23**	3.70	2.90
Triton X-100	**6**	**23**	2.50	2.91
Triton X-100	**28**	**23**	9.90	6.61
Triton X-100	**31**	**23**	4.90	1.70
Triton X-100	**27**	**23**	9.90	5.85

3.3.4.3.2 H^+-driven gates using 4-octylphenol (28)

Tertiary amines are not the only receptors for protons and another class, the phenolates, are able to achieve this too. It is known that phenolates, but not phenols, quench the fluorescence of tris(bipyridyl)Ru(II) via the PET mechanism [86, 87]. Intramolecular cases are also known [88]. No quenching of the fluorophore is observed when the pH is low and the phenoxide group is protonated, while at high pH values the more electron-rich phenolate moiety quenches the fluorescence. When using the lipophilized phenol moiety, 4-octylphenol **28** in SLS with **2,** and also **22**, a full switch was unable to be observed owing to the high pH values needed for full deprotonation of the phenol in the anionic surfactant. A pK_a value of 12.2 was estimated for 4-octylphenol **28,** when associated with both **21,** and **23,** in SLS. The extreme nature of the pK_a value makes it difficult to measure the pH with a glass electrode, given its alkaline error [89]. Once the surfactant was changed to the non-ionic Triton X-100 a significant increase in the FE was obtained to 6.6, while the pK_a value was found to be 9.9. In the case of phenolate receptors, due to their charge they are destabilized by the lower polarity of the Triton X-100 surfactant. The protonated form, the phenol, has no such problem. Hence,

neutral surfactants increase the basicity of the phenolate receptor i.e. pK_a values are raised when compared to water[83]. In the present case, this is not borne out since the pK_a value of a model receptor, 4-methylphenol is 10.2[85], though the difference is close to experimental error.

3.3.4.3.3 H^+-driven gates using 4-tert-butylphenol (27)

4-tert-butylphenol **27** appeared sufficiently hydrophobic to be able to reside in surfactants even in its anionic form. The results show a pK_a of 9.9 was obtained for 4-tert-butylphenol **27** in the presence of **23** and Triton X-100, with a FE value of 5.9. The pH dependence of the fluorescence spectra of **23** with 4-tert-butyl phenol **27** and Triton X-100 is shown in Figure 3.9.

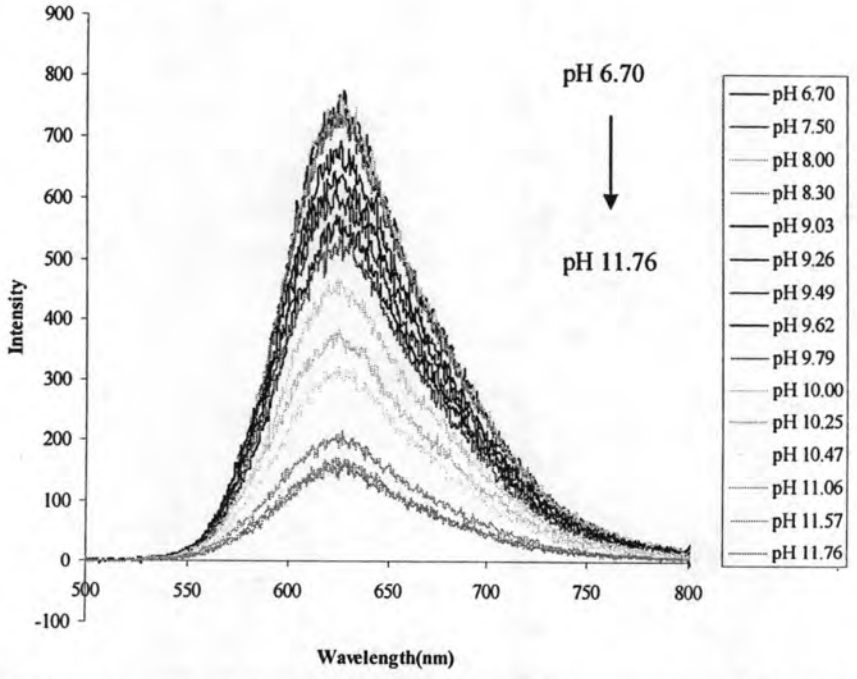

Figure 3.9 Fluorescence spectra of **23** and 4-tert-butylphenol **27** ($1 * 10^{-3}$ M) in Triton X-100 solution as a function of pH (λ_{ex} = 450 nm, λ_{em} = 620 nm) (YES gate).

From all the surfactant-bound receptors for H^+, it was found that 4-octylphenol **28** and 4-tert-butylphenol **27** performed the best in Triton X-100 with good FE values showing YES logic gate action.

3.3.4.4. NOT logic gate

3.3.4.4.1 H^+-driven gates using 4-octylpyridine (30)

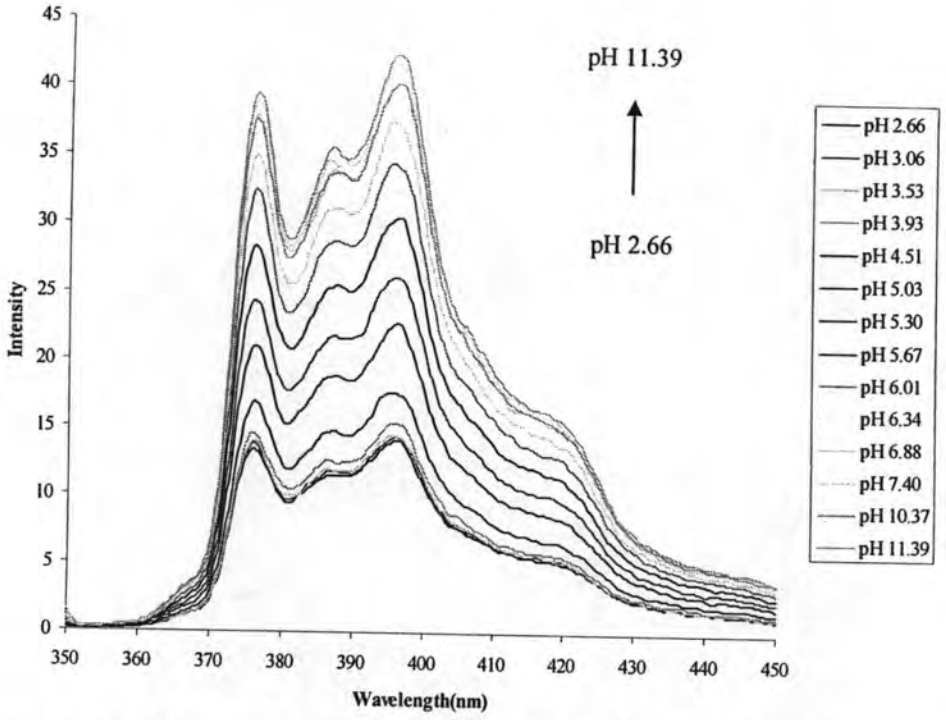

Figure 3.10 pH titration with 4-octylpyridine (1 * 10^{-3} M) and Pyrene in Triton X-100

Owing to its rather low hydrophobicity, 4,4'-bipyridine **31** is not strongly associated with SLS surfactants and probably locates in the bulk water phase. However, when protonated, it will be elctrostatically bound to the anionic headgroups. The cationic tris(bipyridyl)Ru(II) **24** will be bound similarly. So the fluorophore and the protonated receptor will be localized close to each other, allowing PET to occur. Thus a H^+-induced fluorescence quenching is seen. The FE value is therefore less than unity 1.07. It is known that 4,4'-bipyridinium ions (and not 4,4'-bipyridine) quench the fluorescence of tris(bipyridyl)Ru(II) **24** in SLS surfactants [90, 91]. From a frontier orbital theory view, this means that an electron from the LUMO of the fluorophore (once excited) is transferred downhill to the LUMO of the protonated 4,4'-bipyridine. This switches fluorescence 'off'. In contrast, the LUMO of the unprotonated 4,4'-bipyridine is too high in energy to accomplish this PET process. So fluorescence is switched 'on'. From the fluorescence intensity-pH profile, a pK_a value of 4.6 was obtained for 4,4'-bipyridine in the presence of Rubyp **21** and SLS. The pK_a value corresponding to diprotonated 4,4'-bipyridine in water is 3.0 [92]. As with amine receptors, anionic surfactants are expected

to give larger pK_a values than those found in water. So the pK_a value of 4.6 in SLS is reasonable.

An experiment was tried with the non-ionic Triton X-100. It was also necessary to replace Normal Rubpy **21** since it is not hydrophobic enough to associate with Triton X-100. So hydrophobic Rubpy **23** was used instead. A FE value of 1.07 and a pK_a value of 4.9 were found. This significant increase as compared to the situation in SLS is difficult to explain. It is also difficult to understand how the diprotonated 4,4'-bipyridine is associated with the Triton X-100 surfactant, though hydrogen-bonding schemes cannot be discounted. Weak dynamic quenching without a self-assembly component is also a possibility.

Another experiment avoided the tris(bipyridyl)Ru(II) **(24)** and used pyrene **(25)** as the fluorophore instead. Also, 4-octylpyridine **(30)** was used as the receptor. The pH titration studies are shown in Figure 3.10. It can be seen that the fluorescence intensity increases with increasing pH.

The pyridine receptor is unable to donate or accept an electron, as far as the excited pyrene is concerned, due to the energies of the corresponding LUMO's being unfavourable. However, upon protonation, the pyridine unit has a low-lying LUMO, so that an electron from the LUMO of the excited pyrene can be easily transferred. Thus fluorescence is switched 'off' in acidic condictions. The rather long excited state lifetime of pyrene permits this PET process to be kinetically competitive with fluorescence within the surfactant. Diaz-Fernandez et. al [77] had previously observed a similar result. The pK_a value of the 4-octylpyridine **(30)** receptor was calculated to be 3.9 and FE is 4.1. This is understandable in terms of the effect of the neutral surfactant when we notice that the pK_a value of the model compound 4-methylpyridine is 6.0 in water [85].

3.3.4.5 OR and AND logic gates

3.3.4.5.1 Attempted H^+-driven YES gates and Na^+-driven YES gates using 2-methoxyphenyl-15-crown-5 ether (3) and 2-octyloxyphenyl-15-crown-5 ether (8)

As indicated above, receptor **3** gave no measurable fluorescence quenching of dinonylbipyridyl,bis(bipyridyl)Ru(II) **23** in Triton X-100 surfactant solution. This could be attributed the poor hydrophobicity of **3** which prevents it from localizing in the surfactant. This explanation seems reasonable since changing the fluorophore to 9-

cyanoanthracene (which has a larger favourable driving force for PET even though the excited state lifetime is much shorter) did not improve the situation. So the more hydrophobic receptor **8** was employed in place of **3**. Still, no measurable fluorescence quenching was found in the case of dinonylbipyridyl,bis(bipyridyl)Ru(II) **(23)**. This seems to be due to the reduced electron richness of **3** as compared to the calcium receptor. So H^+-driven or Na^+-driven gates could not be attempted in these cases.

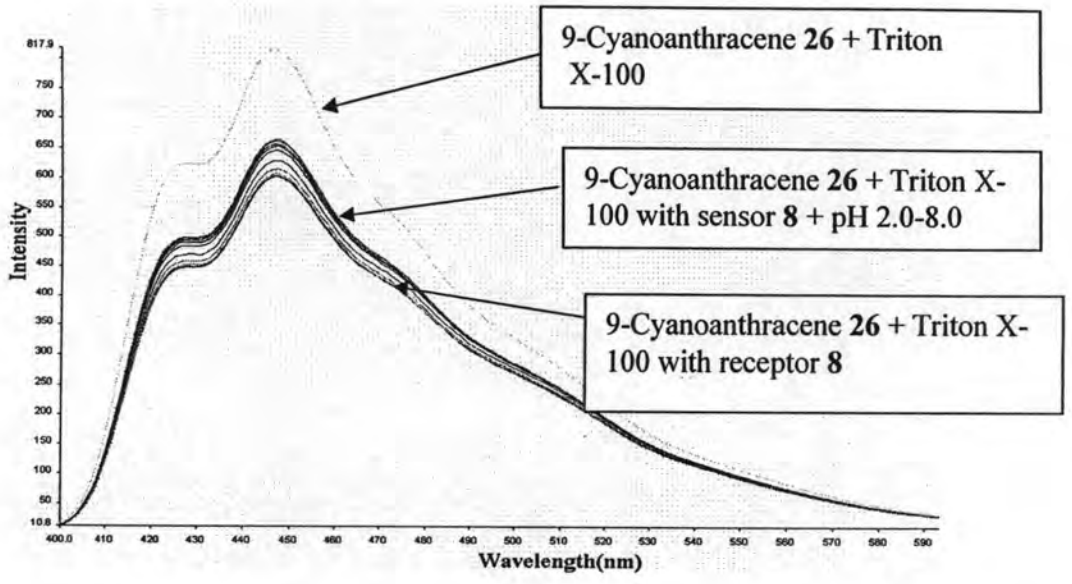

Figure 3.11 Fluorescence spectra of 9-cyanoanthracene **26** and **8** ($1 * 10^{-3}$ M) in Triton X-100 solution as a function of pH (λ_{ex} = 370 nm, λ_{em} = 448 nm) (attempted H^+-driven YES gate).

The experiments with 9-cyanoanthracene fluorophore **26** and the receptor **8** in Triton X-100 surfactant solution are described below. Receptor **8** was employed in pH titration studies from pH 2.0 to 7.0, with Triton X-100 as the surfactant solution and **26** as the fluorophore as shown in Figure 3.10. At low pH, the intensity will be enhanced due to blocking of the PET process arising from the nitrogen center to the fluorophore. At high pH, the fluorescence intensity will be quenched. The pK_a value of the receptor **8** was calculated to be 4.5 and FE is 1.2. The receptor **3** is found within PET sensors [99]. The pK_a value is 5.5 in this case. These two pK_a values are reasonably close, given the fact that Triton X-100 surfactants tend to reduce the pK_a values of amines as compared to the value in water [84]. So, self-assembled 'plug and play' systems show some modular behaviour by approximately preserving the receptor binding properties. But this system involving **8** is not a good H^+-driven YES gate because of the rather small FE value, in this

case stemming from the short fluorescence lifetime of the 9-cyanoanthracene **(26)** fluorophore. Receptor **8** was designed to be selective towards Na^+. So Na^+ variation studies were conducted using various concentrations from 0 M to 1.0 M while holding pH constant at 7.0. The fluorescence intensity – pNa data can be analyzed by a corresponding version of equation (2). The ion-binding constant is given as logβ. The log β value of receptor **8** is 0.06 and the FE value is 1.2.

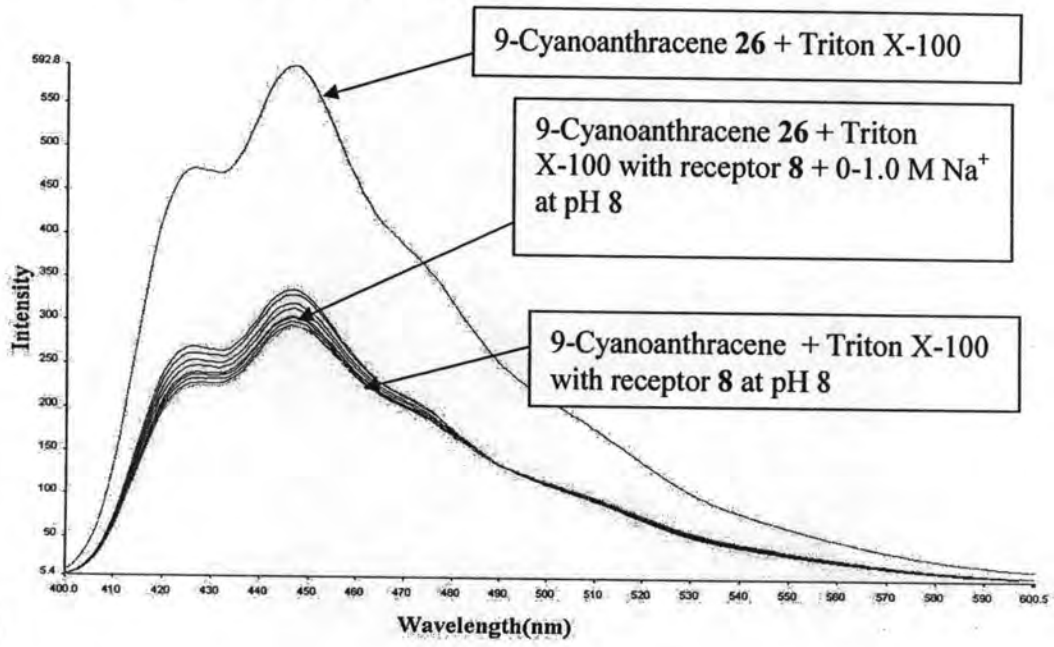

Figure 3.12 Fluorescence spectra of 9-cyanoanthracene **(26)** and **8** ($1 * 10^{-3}$ M) in Triton X-100 solution as a function of $[Na^+]$ (λ_{ex} = 370 nm, λ_{em} = 448 nm) (attempted Na^+-driven YES gate).

Known PET sensors containing the receptor **3** can be considered as a suitable model [100]. The logβ value is 0.9 in this case in neat water. Again, when we allow for the micellar effect, the assembled 'plug and play' system involving **8** has a logβ value rather similar to that of the model. As with the H^+ experiments above, this shows that self-assembled 'plug and play' systems are demonstrably modular since the receptor binding properties are conserved to a significant extent. This is a nice result. But the Na^+-driven YES gate properties of this system involving **8** are not useful because of the rather small FE value, for the same reason as discussed above concerning the H^+-driven case.

Overall, the experiments with the crown ether receptors selective for Na^+ were noticeably less efficient than the N-phenyliminodiacetate receptor selective for Ca^{2+}.

Nevertheless, some interesting comparisons of binding constants of model compounds could be made, to strengthen the expected modularity of self-assembled systems.

3.3.4.5.2 H^+-driven gate using *N,N*-di(carboxymethyl)amino-2-(octyloxy) benzene (10)

Receptor **10** was employed in pH titration studies from pH 2.5 to 10.2, with Triton X-100 as a surfactant and **(23)** as the fluorophore as shown in Figure 3.13. At low pH, the intensity will be enhanced due to blocking of the PET process arising from the nitrogen center to the fluorophore. At high pH, the fluorescence intensity will be quenched. The pK_a value of the receptor **10** was calculated to be 5.9 and FE is 6.7.

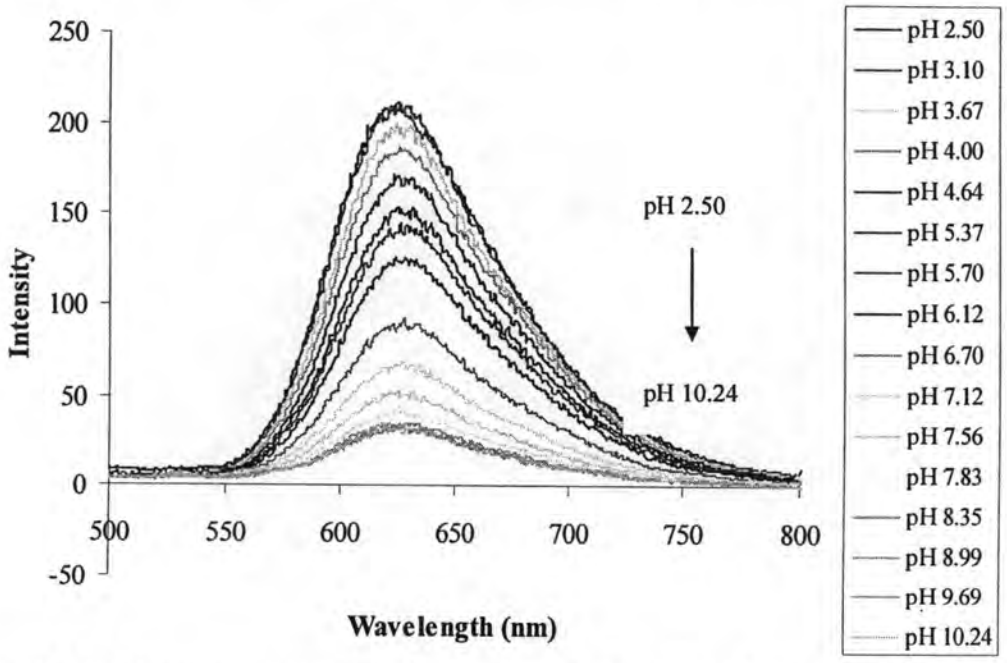

Figure 3.13 Fluorescence spectra of hydrophobic RuBpy **23** and **10** ($1 * 10^{-3}$ M) in Triton X-100 solution as a function of pH (λ_{ex} = 450 nm, λ_{em} = 620 nm) (YES gate).

3.3.4.5.3 Ca^{2+}-driven gate using *N,N*-di(carboxymethyl)amino-2-(octyloxy) benzene (10)

Since receptor **10** was designed to be selective towards Ca^{2+}, calcium variation studies were conducted using various concentrations from 0 M to 0.8 M while holding pH constant at 7.0. The fluorescene intensity –pCa data can be analyzed by a corresponding

version of equation (2). The Ca^{2+}-binding constant is given as log β. The log β value of receptor **10** is 1.6 and the FE value is 2.2.

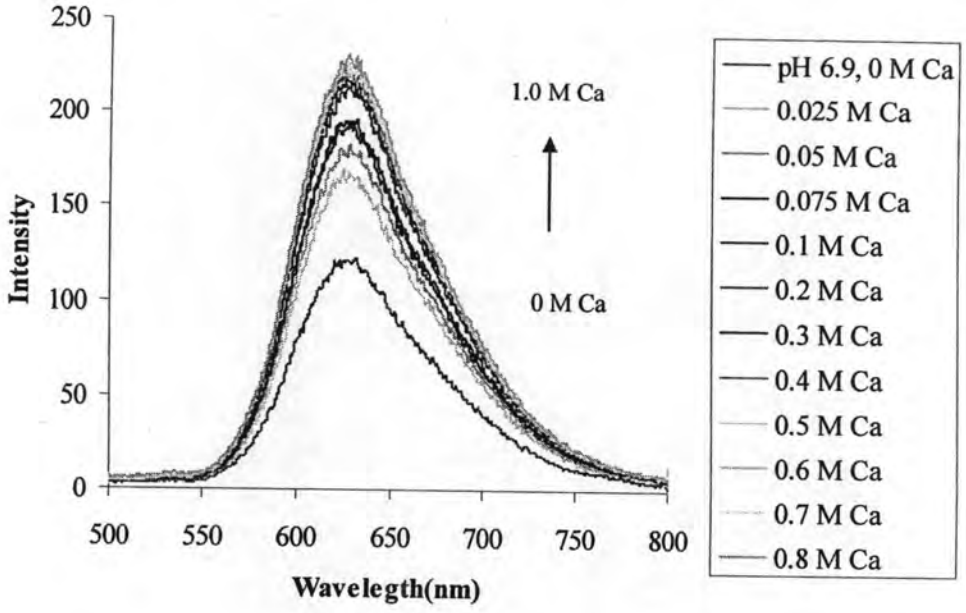

Figure 3.14 Fluorescence spectra of Hydrophobic RuByp **(23)** and **10** (1 * 10^{-3} M) in Triton X-100 solution as a function of [Ca^{2+}] (λ_{ex} = 450 nm, λ_{em} = 620 nm) (Ca^{2+}-driven YES gate).

3.3.4.5.4 OR logic gate

Since receptor **10** was successfully tested under two regimes to bind H^+ and Ca^{2+} separately, we can exploit this non-selectivity to demonstrate OR logic gate action. The first well-behaved molecular OR logic operation was demonstrated within covalently connected fluorophore-receptor systems by exploiting non-selectivity of the receptor [93]. The choice of the 'high' and 'low' levels of the inputs are crucial for this experiment. These are given in Table 3.2. Given its pK_a value of 5.9, a solution of pH 8 (the 'low' value of H^+) will not protonate receptor **10**, but a solution of pH 3.5 (the 'high' value of H^+) will. Triton X-100 was the surfactant, Hydro RuBpy **(23)** was the fluorophore. The conditions for testing the OR logic gate are shown in Table 3.3 and the results are shown in Figure 3.15.

Table 3.2 The condition to specific values for OR logic

	$[H^+]$	$[Ca^{2+}]$
High (1)	$10^{-3.5}$	0.2
Low (0)	$10^{-8.0}$	0.0

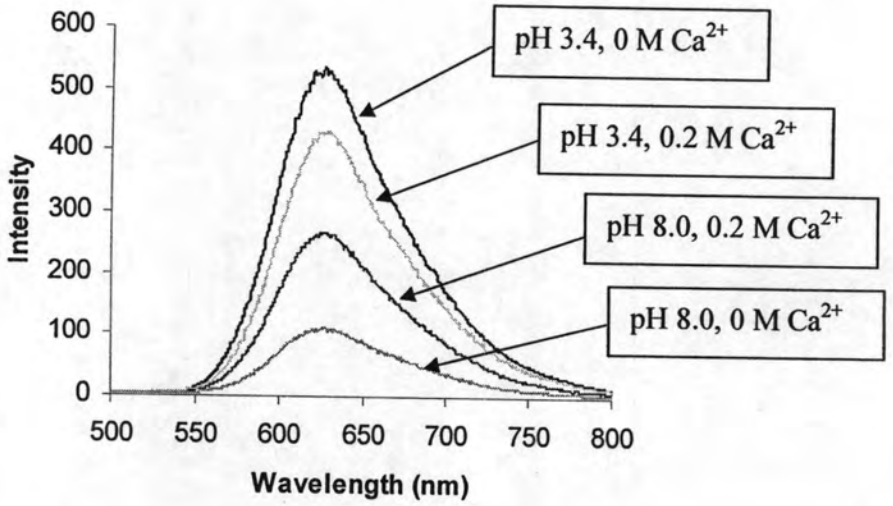

Figure 3.15 Fluorescence spectra of hydro RuByp **23** and receptor **10** ($1x10^{-3}$ M) in Triton X-100 (λ_{ex} = 450 nm, λ_{em} = 620 nm) under various conditions testing H^+, Ca^{2+}-driven OR logic action.

Table 3.3 Operating conditions of **10** for OR logic

Input$_1$ $[H^+]$	**Input$_2$** $[Ca^{2+}]$	**Output** **FE**
$10^{-8.0}$	0.0	1.0
$10^{-3.5}$	0.0	4.7
$10^{-8.0}$	0.2	3.9
$10^{-3.5}$	0.2	2.4

An ideal OR logic gate should have had just one 'low' output signal when both inputs were 'low'. The current results can be viewed successfully since the correct 'low' output is clearly smaller (by a factor of at least 2.4) than the other three. However, the

three 'high' output signals differ among each other by a factor of 2, which is not ideal. The presence of a 'high' level of Ca^{2+} which switches 'on' the fluorescence of the system at pH 7 (as seen in the previous section) and at pH 8 (third entry in Table 3.3) is poorer at doing so at pH 3.5. This is expected from the competitive binding of H^+. However, any copies of receptor **10** which were then protonated were expected to switch 'on' fluorescence of the system just as efficiently (second entry in Table 3.3). It is not clear why this was not seen. Nevertheless, we can be pleased that a satisfactory OR logic action is available from this experiment.

3.3.4.5.5 AND logic gate

Perhaps the most important experiment in this series was to demonstrate that the self-assembly approach could achieve an AND logic gate. After all, the AND logic operation was the first molecular logic action to be published [94]. Also, the AND logic operation requires the selective behaviour of two receptors, each towards its own guest. This experiment used 4-tert-butylphenol **(27)** to provide the H^+ receptor and receptor **10** as the Ca^{2+} receptor without cross-reactivity. The wide separation of the two pK_a values on the pH scale (9.9 and 5.9 respectively) was an important consideration in choosing these two receptors for the experiment. So a solution of pH 8 (the 'high' value of H^+) would serve to protonate the anion of 4-tert-butylphenol **(27)** but not receptor **10**. Similarly, a solution of pH 12 (the 'low' value of H^+) would not protonate either receptor. Triton X-100 was the surfactant and Hydro RuByp **(23)** was the fluorophore. The conditions for testing the AND logic gate are shown in Table 3.4 and the results are shown in Figure 3.16.

Table 3.4 The condition to specific values for AND logic gate

	pH	**$[Ca^{2+}]$**
High (1)	$10^{-8.0}$	0.2
Low (0)	$10^{-12.2}$	0.0

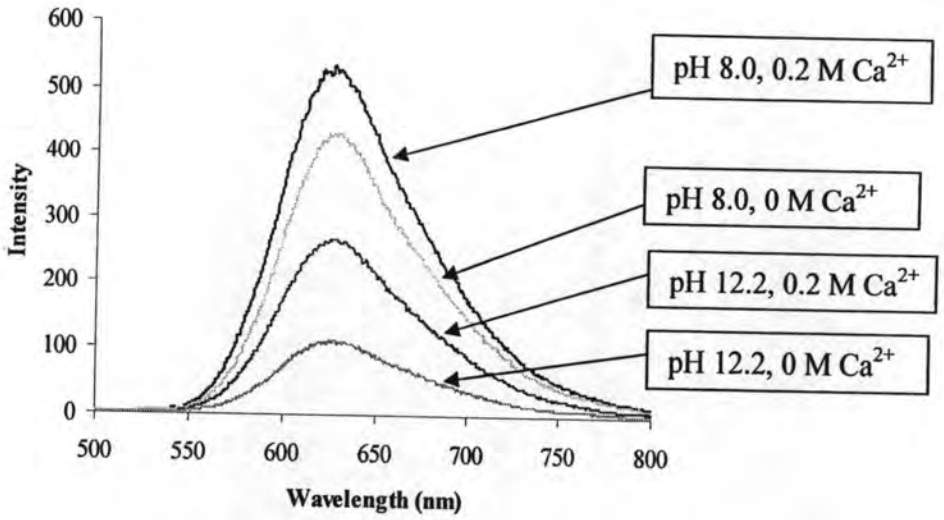

Figure 3.16 Fluorescence spectra of hydro RuBpy **23**, 4-tert-butyl phenol **27** ($1 * 10^{-3}$ M) and receptor **10** ($1 * 10^{-3}$ M) in Triton X-100 ($\lambda_{ex} = 450$ nm, $\lambda_{em} = 620$ nm) under various conditions testing H^+, Ca^{2+}-driven AND logic action.

It is clear that a 'high' fluorescence signal is obtained only when the H^+ input is 'high' (pH 8) and the Ca^{2+} input is 'high' (0.2 M). This 'high' output signal is higher by a factor of at least 2.4 than those found for the other three input combinations. The FE values are given in Table 3.5 in the form of a truth table. Therefore, the AND logic gate experiment has clearly succeeded. However, the result is not ideal since the three 'low' fluorescence outputs are not close to zero, suggesting that the rates of PET are not high even when the receptors are guest-free. This must be related to two facts: (a) the surfactant is a rather large space compared to molecular diameters so that the fluorophore-receptor separation distance is not small enough [81] and (b) the surfactant interior is not polar enough [95].

Nevertheless, this experiment shows the success of the 'plug and play' approach. Indeed, a surfactant solution (PASS 0 logic) was converted to a PASS 1 logic gate by simply adding a fluorophore to the starting solution. This was further converted to a YES gate by adding a receptor to the solution. The choice of the receptor determines the input driving the gate, e.g. H^+ or Ca^{2+}. If the receptor is operated in a non-selective regime by carefully choosing input levels, an OR gate is obtained. The YES gate situation was converted even further to an AND gate by adding in a second receptor. Such a production of a series of molecular logic gates by simply adding extra components is unprecedented.

Table 3.5 Truth table for H^+, Ca^{2+}-driven AND logic in the self-assembled system composed of Hydro RuByp **(23)**, 4-t-butyl phenol **(27)** and receptor **10** in Triton X-100 (λ_{exc} = 450 nm, λ_{em} = 620 nm).

Input$_1$ $[H^+]$	**Input$_2$** $[Ca^{2+}]$	**Output** **FE**
$10^{-12.2}$	0.0	1.0
$10^{-8.0}$	0.0	3.8
$10^{-12.2}$	0.2	2.7
$10^{-8.0}$	0.2	9.2

3.3.5 The results and discussion for molecular logic gates on beads

The previous section has clearly demonstrated the aims of this project and has given an explanation of the theories and mechanisms that occur. This chapter aims to utilise our understanding of these mechanisms by obtaining unequivocal results. Although the main objective of this project is to analyse the behaviour of logic gates on beads, the following results are based on pyrazoline logic gates in solution phase only. Measurements for logic gates in the solid phase will be carried out in the near future.

3.3.5.1 Synthesis of pyrazolines

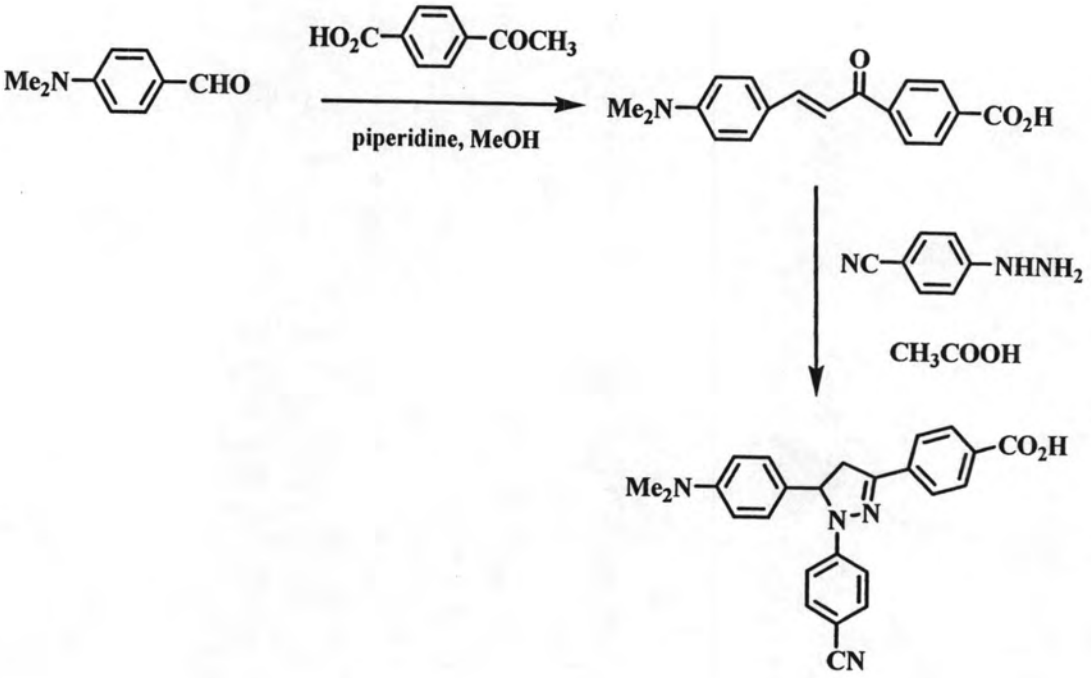

12b

The *(E)*-4-(3--(4(dimethyamino)phenyl)acryloyl)benzoic acid **12)** was formed by condensation of 4-(dimethylamino)benzaldehyde and 4-acetylbenzoic acid using piperidine and dissolved in dry methanol. The pyrazoline was then formed via cyclisation using 4-cyanophenyl hydrazine hydrochloride dissolved in boiling acetic acid.

3.3.5.2 H^+ Titration of Molecule 12b

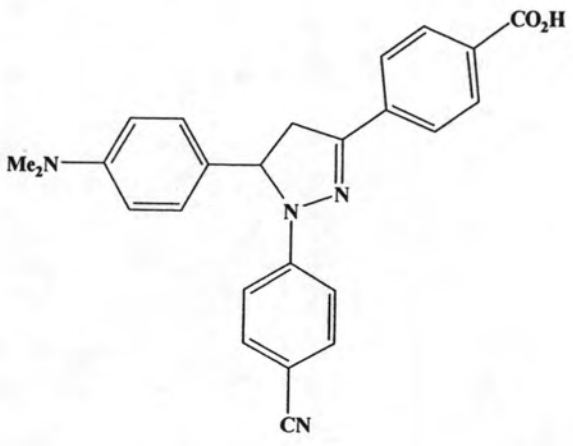

The spectral properties of pyrazoline **12b** were investigated in a MeOH/H_2O (20:80) solution using aliquots of H_3PO_4 and NaOH to adjust pH. A pH range 2.0-9.1 was investigated using in a 2.5 * 10^{-6}M solution. The spectral data displayed in Figure 3.17 show the behaviour of the molecule during the titration.

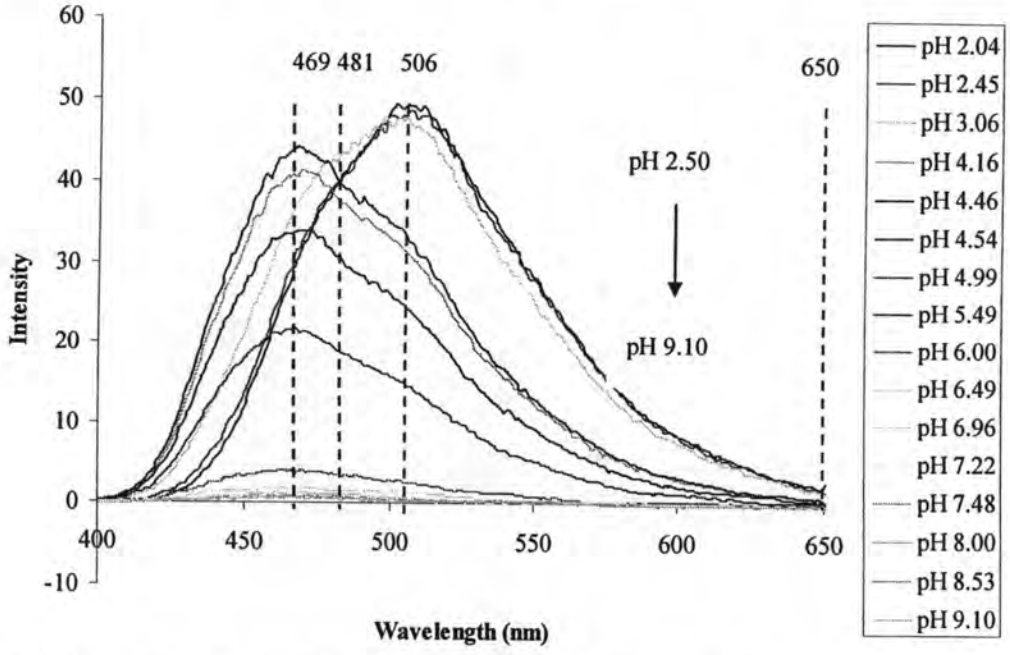

Figure 3.17 Emission spectra of pyrazoline **12b** upon pH variation

When the spectral data of pyrazoline **12b** is contemplated reveals that it can be a fairly flexible logic gate, being able to perform a number of Boolean functions depending on which wavelength is chosen to be monitored. For example in Figure 3.17 it can be seen that the molecule behaves as a YES gate at the wavelengths 506, 481 and 469 nm. The intensity curves at low pH values are much greater than that of high pH values, which barely move away from the base line. This is classic 'on/off' switching behaviour and occurs when protons are complexed with the amine receptor, perturbing PET and allowing fluorescence to occur relatively unhindered. If we consider protons as an input (1) and the high intensity of fluorescence as an output (1) then it can be seen that **12b** behaves as a YES gate. The logic gate reveals a further Boolean operation when another wavelength is considered. For example intensities at 650 nm demonstrate good PASS 0 behaviour as no matter what the pH fluorescence is always switched 'off. However, PASS 0 is considered to be trivial in semiconductor computing, but has uses in MCID.

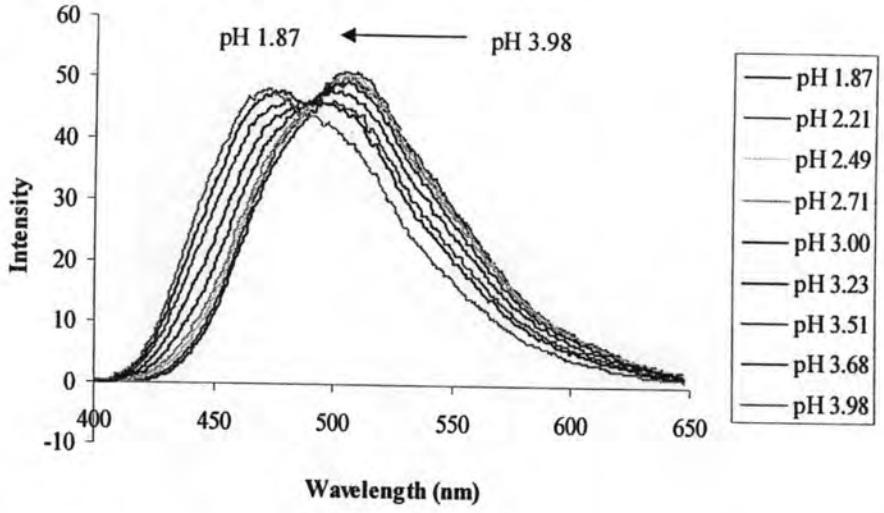

Figure 3.18 Emission spectra of **12** upon pH variation at the point of wavelength shift

In Figure 3.18 it is clear that there is a blue shift from 506 nm to 469 nm in the spectra. This is shown in more detail in a further titration shown in Figure 3.18. An explanation for this wavelength shift is intramolecular charge transfer (ICT). ICT occurs when the charge density within the excited molecule is redistributed. Charge density can be disturbed in a couple of ways, for example one of the main contributors to a wavelength shift is the solvent. Polar solvent molecules can interact with **12** to stabilise its internal charge. Figure 3.19 illustrates this effect with peak wavelengths measuring at 454 nm for toluene, 467 nm for THF and 507 nm for MeOH/water. Testing the molecule in different solvents is further evidence of an ICT system within this compound. Another situation in which a wavelength shift can be brought about is when the molecule interacts with a guest species, especially a charged ion. In our case, the cause of the blue shift is the deprotonation of the carboxylic acid at higher pH values, illustrated in Figure 3.20.

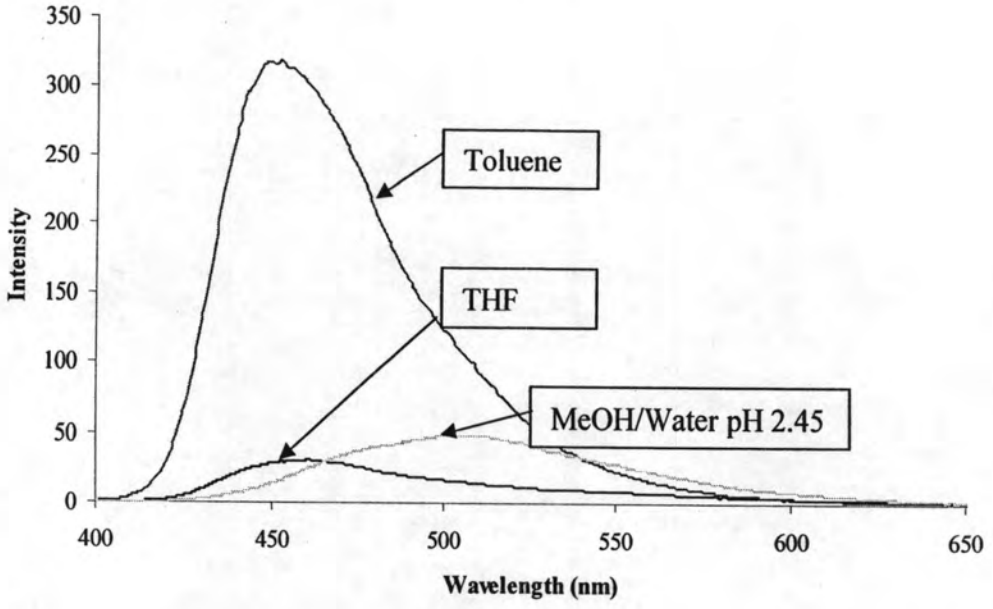

Figure 3.19 Evidence of ICT and wavelength shifts in different solvents of molecule **12**

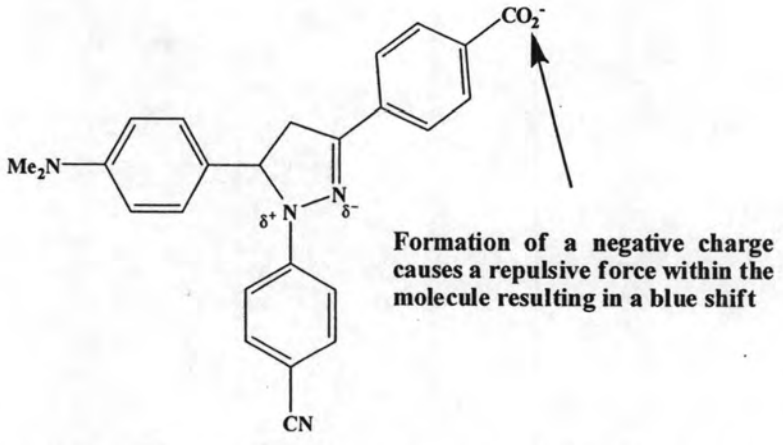

Figure 3.20 Deprotonation of the carboxylic acid group in the ICT excited state of **12b**

pK_a values of 4.8 and 4.5 were calculated for **12b** corresponding to the amine receptor and the CO_2H receptor respectively by using a version of equation (1.2).

It can be useful to know the binding constant for the H^+ of a given logic gate. The binding constant can be defined as the point at which the intensity of the fluorescence is exactly half that of maximum intensity for that wavelength i.e. it is the point at which the switch is 'half on, half off'. Binding constants of pK_a=4.8 and pK_a=4.5 have been

calculated for molecule **12b** corresponding to the amine receptor and the CO_2H receptor respectively.

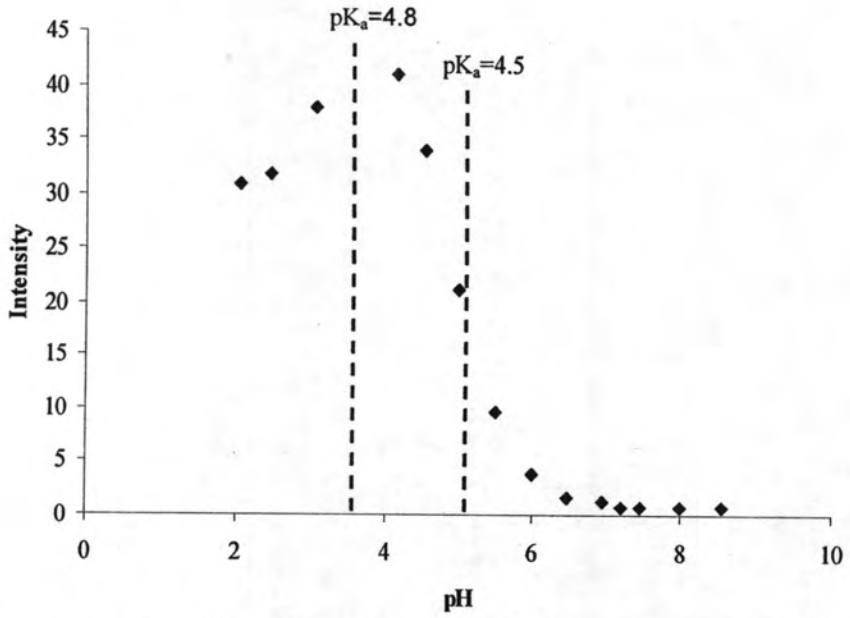

Figure 3.21 Graph showing the similar binding constants at two stepping regions of the intensity at 470 nm vs pH plot

3.3.5.3 H^+ Titration of Molecule 13b

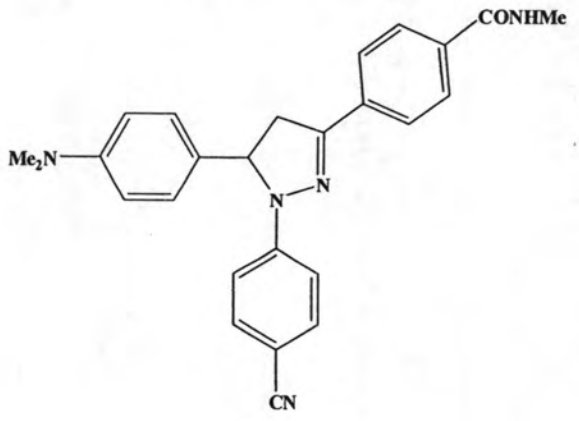

The spectral data displayed in Figure 3.22 illustrate the behaviour of **13** during titration.

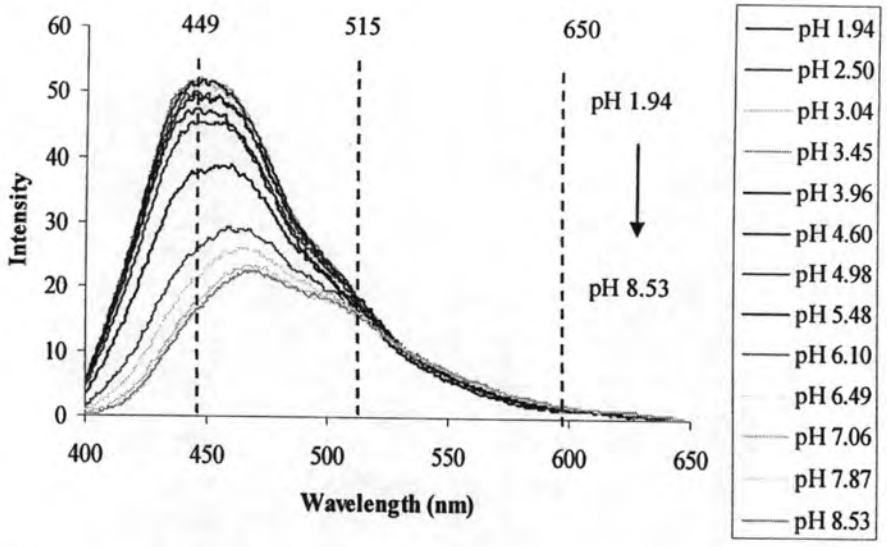

Figure 3.22 Emission spectra c **Wavelength (nm)**

The spectra show that as pH increased the intensity of fluorescence emission decreased. The pK_a value is calculated as 5.5. Just like **12b** , **13b** displays the behaviour of more than one Boolean function. In similar to **12b**, when fluorescence at 449 nm is monitored it can be seen that the switching behaviour is indicative of a YES gate. 515 nm would be another useful wavelength for the use of a PASS 1 and once again 650 nm picks out a PASS 0 region.

3.3.5.4 H^+ Titration of bead 12b

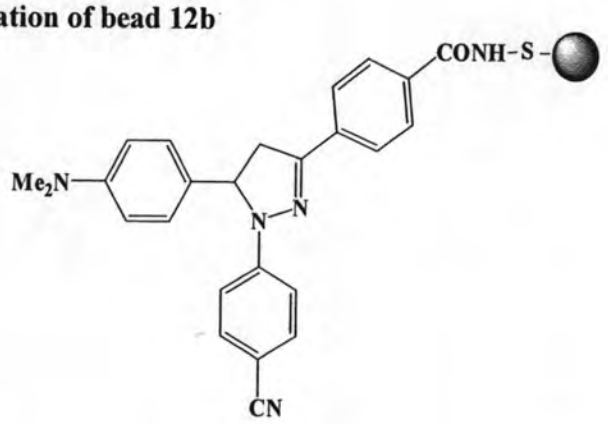

Aminopropylsilica beads in DMF were reacted with **12b** with the aid of HOBT and DIC. The beads were washed to remove unreacted materials. Then, the **bead 12b** was studied by fluorescence during H^+ titration.

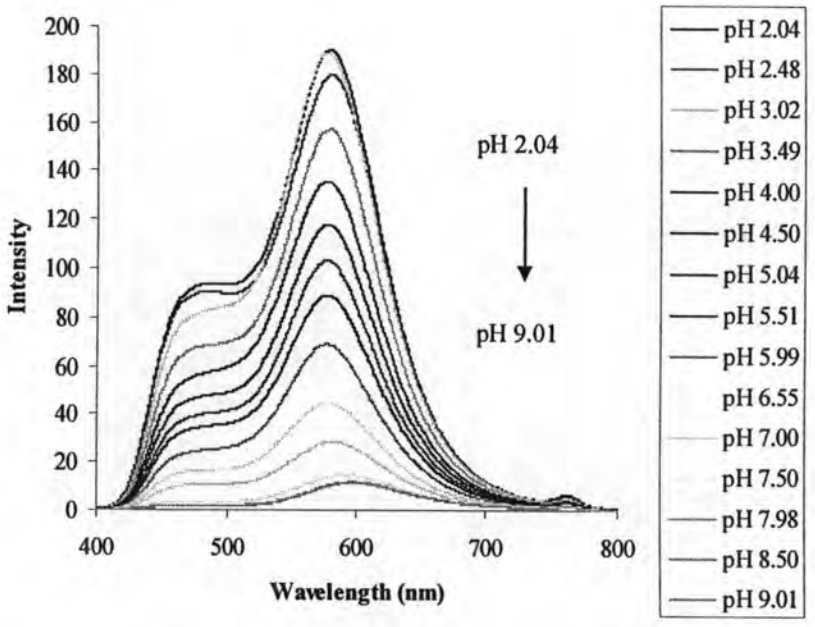

Figure 3.23 Fluorescence spectra of **bead12b** in methanol:water (1:1) solution as a function of pH (λ_{exc} = 380 nm).

An important aim of this work was to test the fluorescence switching properties of these pyrazolines once they were immobilized on beads. This would be useful to produce re-usable fluorescence sensor particles. Perhaps more importantly, this would be useful to produce tags which identify small objects even in large populations. The method of molecular computational identification (MCID) was proposed recently.[97] Besides these applications, it would be very interesting to observe the influence of the bead surface environment on the bound switch molecules. The fluorescence spectra of bead **12b** as a function of pH is shown in Figure 3.23. It is immediately apparent that major changes have occurred in the shape of the spectra. Besides the expected band at 470 nm, there is a larger band at 575 nm. The latter band is due to excimer formation. This is the association between an excited fluorophore and another ground state fluorophore, which is enabled by the relative closeness of the switch molecules bound to the bead surface. When the total area of each spectrum is plotted against its corresponding pH (Figure 3.25) a stretched sigmoidal curve is found. The reason for the stretching beyond the normal pH range of 2 units is that the bead surface presents a dispersion of environments for the switch molecules to reside in. Therefore each population of switches will have its own characteristic pK_a value. The overlap of these produces the stretching observed. Such overlapping of different switches with different pK_a values can give very wide dynamic

ranges.[98] The FE value is 19.4. It is notable than the solution-based experiments for the model pyrazoline **12b** gave a much smaller FE value. This suggests that the significant aggregation effects seen for these rather hydrophobic pyrazolines in solution phase which reduced PET rates, can be avoided by dispersal and immobilization on the aminopropylsilica (APS) surface. It is clear that the two emission bands behave somewhat differently in terms of the FE values at a given wavelength and also in terms of the pH-dependence of the band maximum wavelengths. Actually, these two effects are related since pH-dependent band maxima require the 'off' state to have sufficient intensity when compared to the 'on' state. So that is why the band at 470 nm which is fully switched 'off' in alkaline solution shows no pH-induced shifts. Why is the emission band at 575 nm showing a smaller, though still large, FE value? The reason is that it is an excimer band whose energy is much less than that of the monomer (i.e. unassociated) band at 470 nm. So, less energy is available to drive the PET process in alkaline solution. When the data in Figure 3.24 were plotted according to equation 2 , a pK_a value of 5.0 is found. For comparison, the precursor pyrazoline **12**b and the model pyrazoline **bead 12b** have pK_a values around 4.5. The bead surface has two effects on the switch pK_a value. First, the lack of mobile dipoles in the bead silica lattice produces a lower polarity as compared to water. This would decrease the pK_a value since the stability of the protonated aniline receptor would be reduced. However, the second effect is due to the electrostatic effect of the $Si\text{-}O^-$ groups on the surface. The effect of these is to concentrate protons and to stabilize the protonated aniline receptors. These two connected effects serve to increase the pK_a value. Evidently, the electrostatic effect is dominant. So, the bead-based work has resulted in interesting differences from the solution experiments, even at this preliminary stage. We can expect more interesting data to emerge when all the pyrazolines are studied fully.

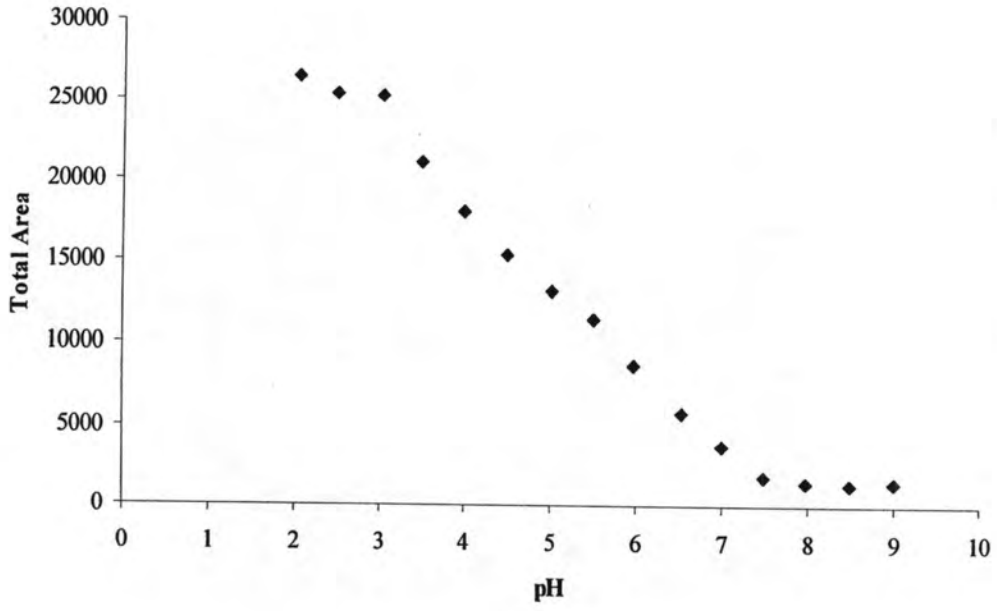

Figure 3.24 Fluorescence spectral area of **bead12b** in methanol:water (1:1) solution as a function of pH (λ_{exc} = 380 nm).

3.3.5.5 H^+ Titration of Molecule 15b

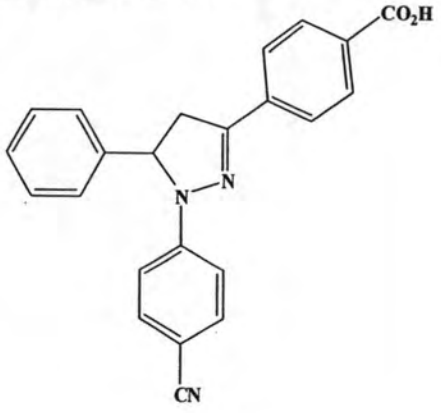

The spectral properties of **15b** were investigated similarly. The spectral data displayed in Figure 3.25 illustrates the behaviour of the molecule. **15b** responded to pH because its CO_2H group contains a receptor (CO_2^-) for H^+. It was found that as the concentration of protons was decreased, the amount of fluorescence increased; in effect **15b** is able to mimic the behaviour of a NOT gate. Once again the molecule is shown to perform a range of Boolean functions. For instance monitoring fluorescence intensity at 462 nm can offer a NOT gate.

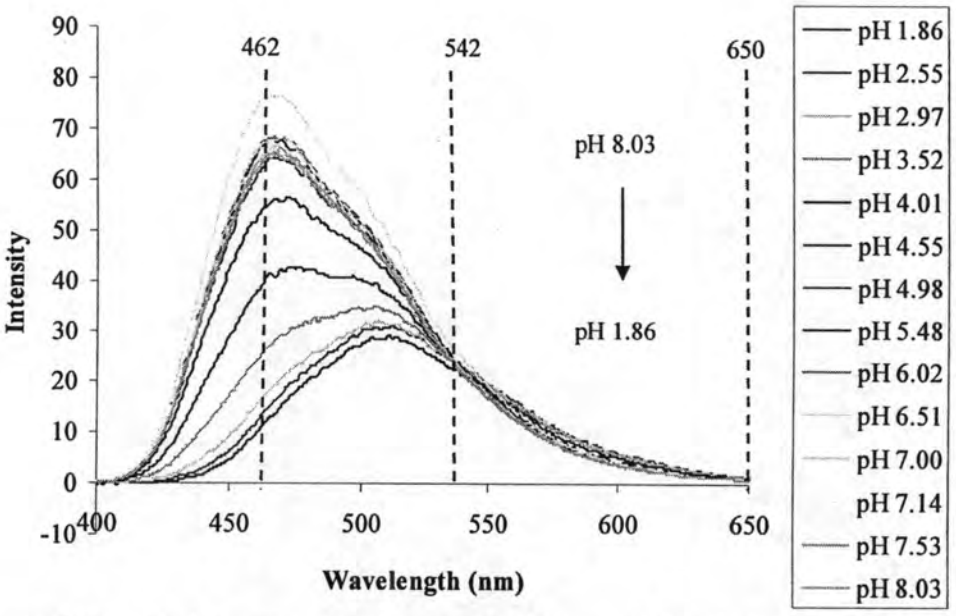

Figure 3.25 Emission spectra of molecule **15b** upon pH variation

Furthermore if fluorescence emission at 542 nm was monitored a PASS 1 would once again become available. Finally intensities at 650 nm offer a PASS 0 gate also. The spectral data in Figure 3.25 clearly displays a H^+ induced red shift which can be explained by the deprotonation of the carboxylic group similar to the case for **12b**. The acidic form of **15b** produces the red-shift i.e. the stabilised ICT state. This state would have the greater degree of ICT which can interact to a greater extent with the solvent via hydrogen bonding. This coupling results in loss of vibrational energy and consequently fluorescence intensity. This is the simplest explanation for the spectral behaviour in Figure 3.28.

3.3.5.6 H^+ Titration of Molecule 16

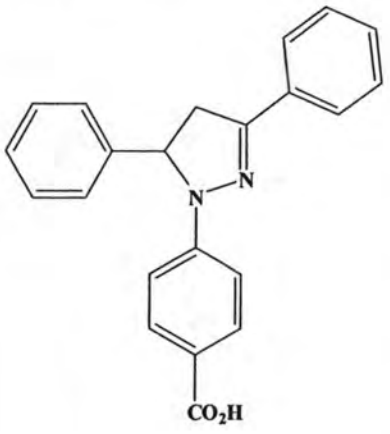

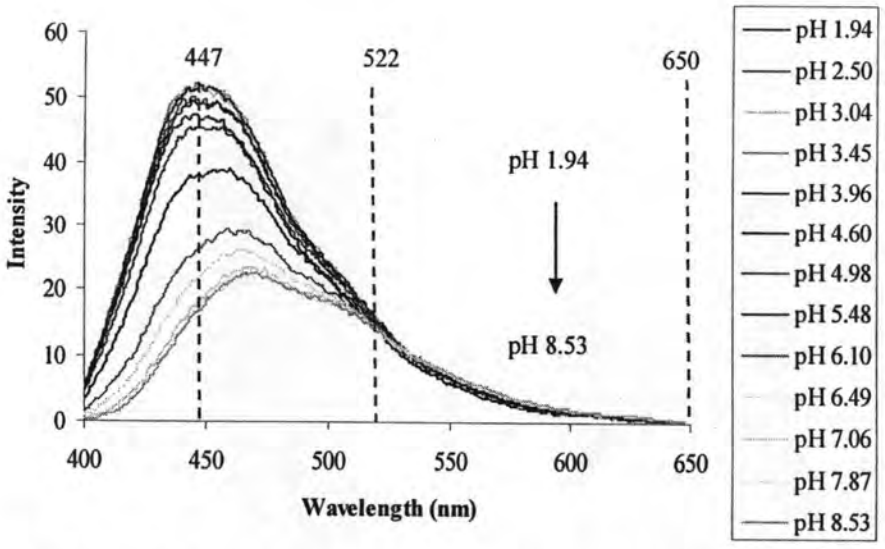

Figure 3.26 Emission spectra of molecule **16b** upon pH variation; pH1.94, 2.50, 3.04, 3.45, 4.60, 4.98, 5.48, 6.10, 6.49, 7.06, 7.84, 8.53

The emission spectra in Figure 3.26 shows that as pH increased the intensity of fluorescence emitted decreases. The pK_a value is calculated as 4.9. When fluorescence at 447 nm is monitored it can be seen that a YES gate is available. At 522 nm fluorescence intensity is approximately the same for all pH values so this can be seen as a PASS 1. Finally the approximately zero fluorescence intensity at 650nm facilitates a PASS 0 gate once again. Figure 3.26 shows a H^+-induced blue shift which can be explained as done for **16b**, except that now the CO_2H group is in a different position of the pyrazoline heterocycle. The basic form of **16b** produces the red-shift. This is the stabilised ICT excited state. So this state would possess the greater degree of ICT, which leads to the greater degree of hydrogen bonding with the solvent. Again loss of vibrational energy is greater here. Hence the basic form of **16b** emits less (than the acidic form).

3.3.5.7 H^+ Titration of Molecule 18b

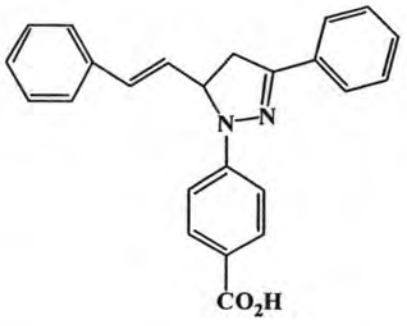

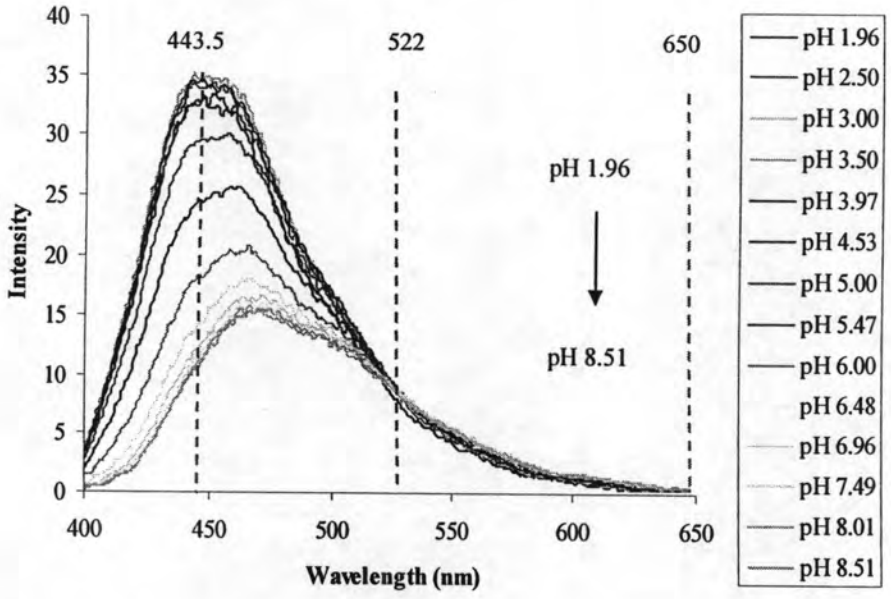

Figure 3.27 Emission spectra of molecule **18b** upon pH variation

From the emission spectra Figure 3.27 shows that as pH increased the intensity of fluorescence emitted decreases. The pK_a value is calculated as 5.6. When fluorescence at 443.5 nm is monitored it can be seen that a YES gate is available. At 522 nm fluorescence intensity is approximately the same for all pH values so this can be seen as a PASS 1. Finally the approximately zero fluorescence intensity at 650 nm facilitates a PASS 0 gate once again. Inspection of **18b** shows it has an extra double bond when compared to **16b**. This feature, in closely related structures, leads thermally assisted photodissociation [96]. So **18b** was studied to explore the effect of temperature on its fluorescence. The preliminary thermal studies of **18b** were in the polar and nonpolar solvent shown in Figure 3.33. The **18b** in nonpolar solvent can give enhancement of fluorescence over in the polar solvent because polar solvent is able to interact with **18b** and stabilize internal charge transfer states. The case of **18b** in hot toluene shows less intensity than in cold because the high temperature causes photodissociation within **18**b.

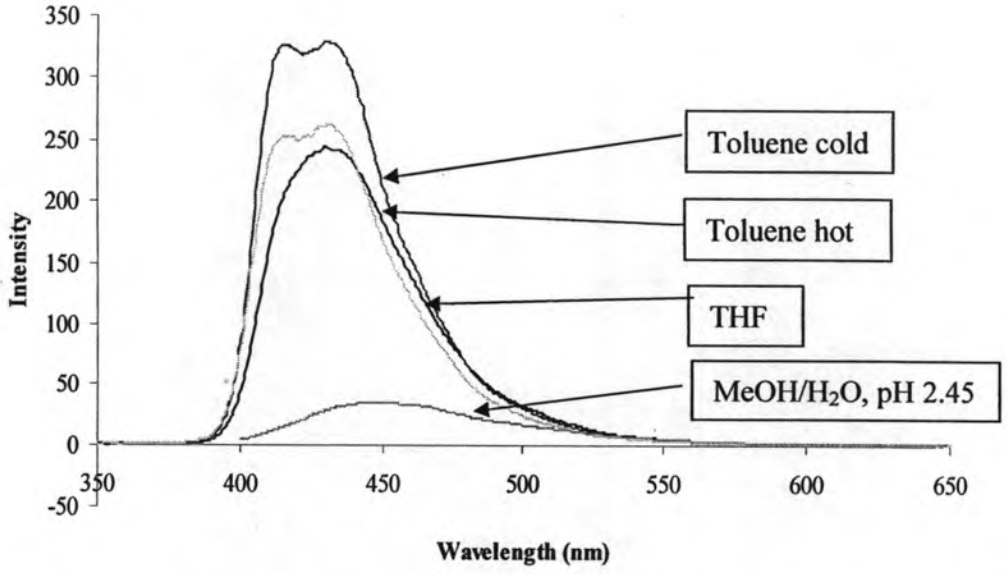

Figure 3.28 Evidence of ICT and wavelength shifts in different solvents of molecule **18b**

3.3.5.8 H^+ Titration of Molecule 20

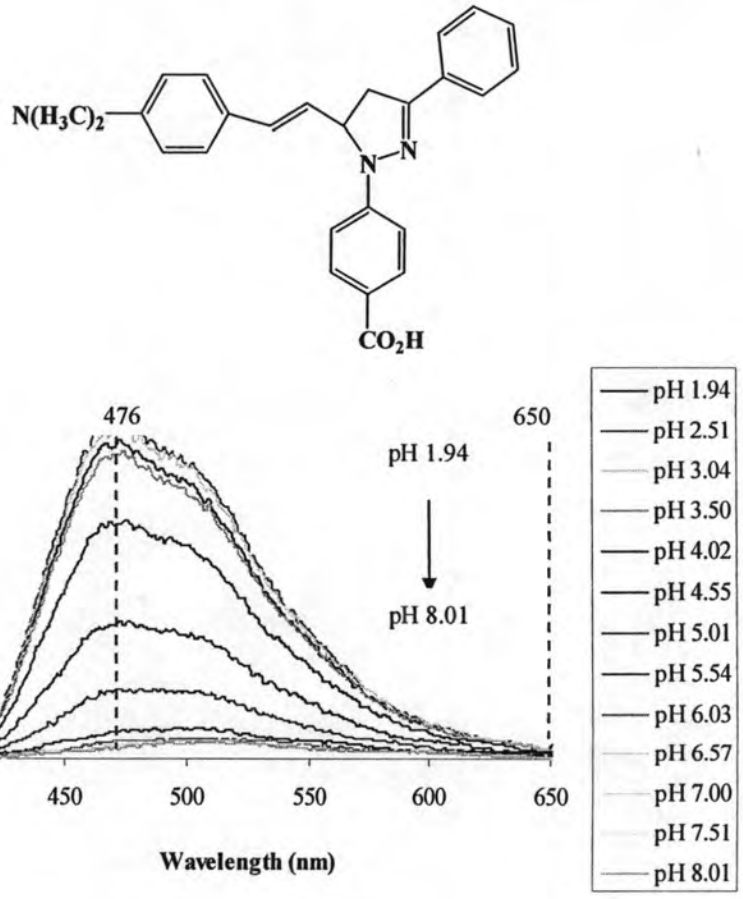

Figure 3.29 Emission spectra of molecule **20b** upon pH variation

From the emission spectra Figure 3.29 shows that as pH increased the intensity of fluorescence emitted decreases. The pK_a value is calculated as 4.4. When fluorescence at 476 nm is monitored it can be seen that a YES gate is available. Finally the approximately zero fluorescence intensity at 650nm facilitates a PASS 0 gate once again. The result of the thermal effect in polar and apolar solvent of **20b** is similar to the study of **18b** shown in Figure 3.30. The polar solvent stabilizes the ICT state and causes the red shift. But in the nonpolar solvent, the emission will be enhanced. The intensity of cold toluene is higher than hot toluene because of the thermally assisted photodissociation.

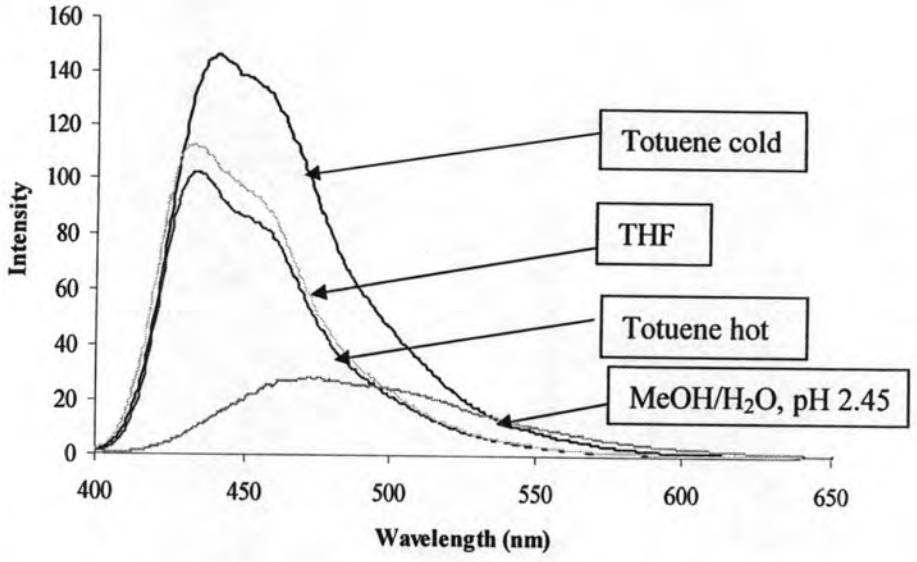

Figure 3.30 Evidence of ICT and wavelength shifts in different solvents of molecule **20b**

Overall, several fluorescent pyrazolines bearing carboxylic acid groups have been prepared and tested in homogeneous solution. This is a necessary preliminary step before immobilizing these compounds on beads. Bead-based experiments are in progress.